UNIVERSITY OF TURKU

# Vimentin in mammary gland morphogenesis and contractility during lactation

Institute of Biomedicine
MDP in Biomedical Sciences, Drug Discovery and Development
Master's Thesis

Author:
Pinja Thorén

Supervisor:
Emilia Peuhu, Docent
Oona Paavolainen, MSc
Institute of Biomedicine

16.12.2022
Turku

The originality of this thesis has been checked in accordance with the University of Turku quality assurance system using the Turnitin Originality Check service.

Master's thesis

**Subject**: Institute of Biomedicine, MDP in Biomedical Sciences, Drug Discovery and Development
**Author**: Pinja Thorén
**Title**: Vimentin in mammary gland morphogenesis and contractility during lactation
**Supervisors**: Docent Emilia Peuhu, MSc Oona Paavolainen
**Number of pages**: 72 pages, 3 appendixes
**Date**: 16.22.2022

The mammary gland becomes fully differentiated upon pregnancy and lactation preparing it for nourishing the offspring. Mammary basal epithelial cells lining the ducts and alveoli contract to propel the secreted milk to the nipple. These cells express vimentin intermediate filaments, which have been shown to be involved in development and regulation of cell mechanical strength and movement. While vimentin deficiency was shown to reduce basal epithelial cell proportion and delay ductal outgrowth during pubertal mammary gland development, little is known about the role of vimentin in the lactating mammary gland. In this research project the role of vimentin in basal cell contractility and lactogenic differentiation was explored. The comparison of lactating mammary gland phenotype in wild type (WT) and vimentin knock-out (*Vim*$^{-/-}$) mice showed no clear differences, but detailed image analysis revealed a large variation in the alveolar size and disorganised morphology in *Vim*$^{-/-}$ mammary gland. While milk lipid droplets were fewer but larger inside lactating *Vim*$^{-/-}$ mammary epithelial cells, the analysis of milk spots and litter weights in the pups of WT and *Vim*$^{-/-}$ dams demonstrated no significant effects on nursing, suggesting that any defects in lactational differentiation are likely compensated with other mechanisms. Furthermore, no consistent changes in the contractile readout, myosin II phosphorylation, upon vimentin silencing or knockout were detected in human and mouse mammary glands, respectively. This might further reflect the adaptive capacity of the organ to sustain the vital function in mammals. Further details of vimentin in mammary gland function might be detected when examining the actively contracting gland.

**Key words**: mammary gland, vimentin, lactation.

# Table of content

**1 Introduction ..... 5**

**1.1 Mammary gland structure ..... 5**

**1.2 Mammary gland cell types and their function ..... 7**

1.2.1 Mammary basal epithelial cells ..... 7

1.2.2 Mammary luminal epithelial cells ..... 9

1.2.3 Other cell types of mammary gland ..... 10

**1.3 Mammary gland development ..... 11**

**1.4 Vimentin ..... 14**

**2 Aims of the research project ..... 18**

**3 Results ..... 19**

**3.1 *Vim*$^{-/-}$ mice do not have obvious defects in nursing capabilities ..... 19**

**3.2 Vimentin deficiency alters the morphology of the lactating mammary gland ..... 20**

**3.3 *Vim*$^{-/-}$ mammary epithelial cells have fewer but larger lipid droplets ..... 24**

**3.4 Non-stimulated mouse mammary gland has little myosin phosphorylation ..... 27**

**3.5 Myosin-light chain 2 phosphorylation does not change consistently in basal mammary epithelial cells upon vimentin knockdown ..... 29**

**4 Discussion ..... 34**

**4.1 Challenges in *Vim*$^{-/-}$ mice breeding might be caused be phenotypes other than defective lactation ..... 34**

**4.2 Vimentin deficiency increases the alveolar size distribution in the lactating mammary gland ..... 35**

**4.3 Vimentin regulates the accumulation of milk lipid droplets in luminal mammary epithelium ..... 38**

**4.4 Myosin-light chain 2 phosphorylation has limited applicability in the analysis of mammary gland contraction ..... 41**

**5 Conclusion ..... 45**

**6 Methods ..... 46**

**6.1 Mice ..... 46**

**6.2 Whole mount staining ..... 47**

**6.3 Immunofluorescence staining of tissue sections ..... 47**

**6.4 Polyacrylamide hydrogel preparation ..... 49**

**6.5 Primary human mammary epithelial cell isolation ..... 50**

**6.6 Lentiviral gene silencing ..... 50**

**6.7 Human mammary epithelial cell immunofluorescence ..... 51**

**6.8 Microscopy ..... 52**

**6.9 Image analysis ..... 52**

**6.10 Statistical analysis ..... 55**

**Acknowledgements ..... 57**

**List of abbreviations ..... 58**

**References ..... 60**

**Appendixes ..... 71**

**Appendix 1: Multiple-comparison p-values of alveoli size per mouse ..... 71**

**Appendix 2: Periodate-Lysine-Paraformaldehyde-buffer recipe ..... 72**

**Appendix 3: P-buffer recipe ..... 72**

# 1 Introduction

## 1.1 Mammary gland structure

Mammary glands are the milk-producing organs found in mammals, and they distinguish mammals from all other animals (Hassiotou & Geddes, 2013; Macias & Hinck, 2012; McNally & Stein, 2017). The milk produced in mammary glands not only nourish the offspring, but also provides important protection against pathogens (Hassiotou & Geddes, 2013). The human mammary gland is divided into 15 to 20 lobes, which are embedded in the adipocyte-rich stroma (Figure 1A) (Hassiotou & Geddes, 2013; Tortora & Bryan, 2014).

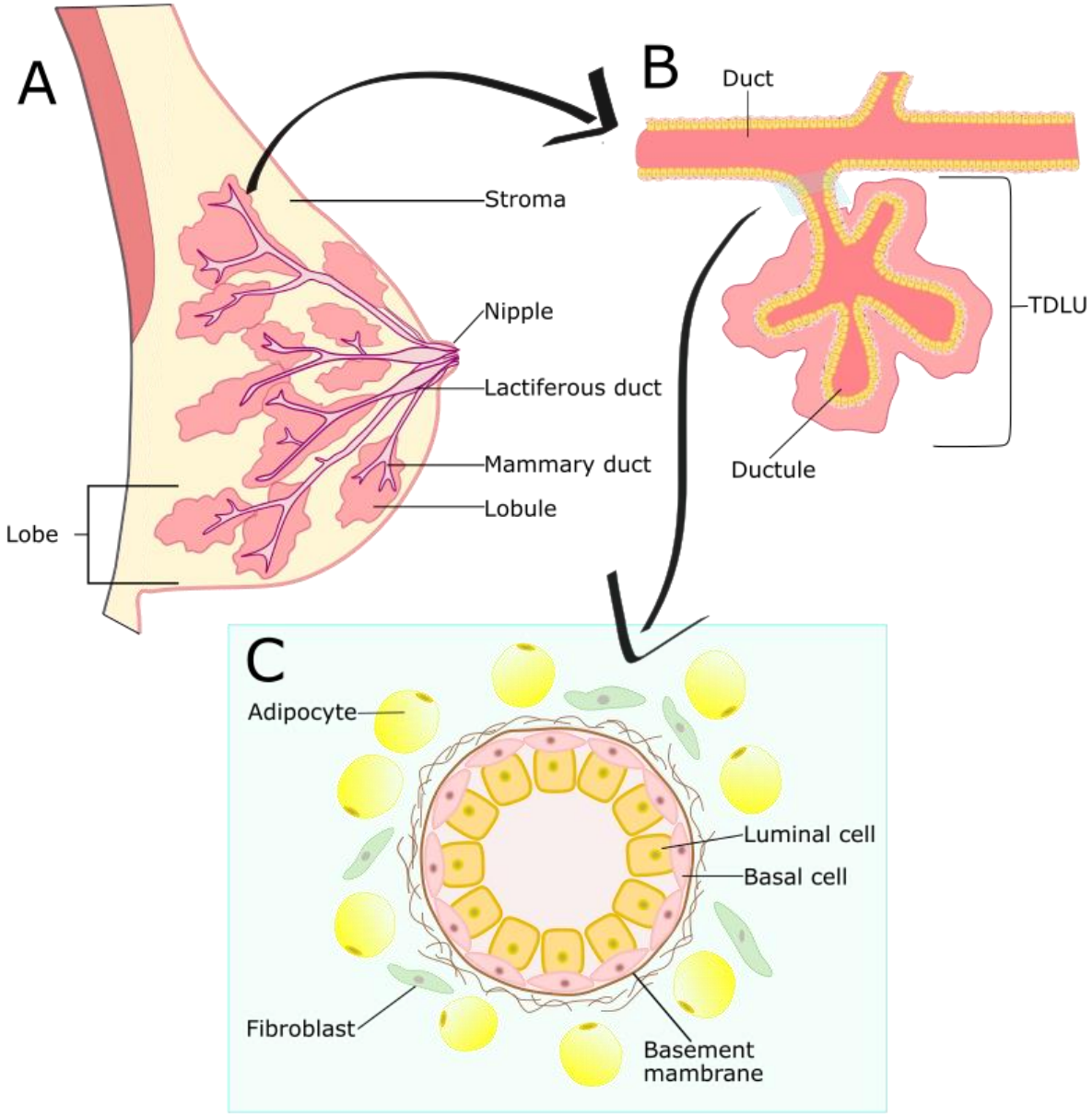


**Figure 1: Overview of human mammary gland structure.** (A) A mammary gland is formed by several lobes containing lobules that drain through a mammary duct to a lactiferous duct, which opens up in the nipple. (B)

Terminal ductal-lobular unit (TDLU) is the functional unit of a mature human mammary gland. (C) Representation of the bilayered structure found in the tubule-alveolar mammary gland epithelium.

Each lobe contains lobules which, in turn, are made up of acini, which differentiate into milk producing alveoli during pregnancy and lactation (Macias & Hinck, 2012; Tortora & Bryan, 2014). Alveoli are drained by ductules that eventually merge into mammary ducts. The functional unit of human mammary gland is terminal ductal-lobular unit (TDLU) (Figure 1B), a group of alveoli that drain to the same duct (McNally & Stein, 2017). Mammary ducts merge to form lactiferous ducts that opens up at the nipple (Tortora & Bryan, 2014). In addition to the supporting stroma, the loose framework of fibrous connective tissue, called Cooper's ligaments, maintain the position of mammary glands within the breast (Cooper, 1840).

Due to limitations in obtaining healthy tissue material, the human mammary gland structure, function and development is not fully determined, and majority of current knowledge arises from research done in rodents. Mice have five pairs of mammary glands (Figure 2A) while humans only have one pair. In structural comparison, an adult virgin mouse mammary gland structure is simpler than in humans, and represents an extensive ductal tree (Figure 2B). Furthermore, while TDLU forms a functional unit in the human breast, comparable structures form in the mouse mammary gland only upon pregnancy and lactation through side branching. On cellular level, human and mouse mammary epithelia is relatively similar (Figure 1C), although cell type specific differences in protein expression and the regenerative capacity have been detected. (Dontu & Ince, 2015; Geddes, 2007)

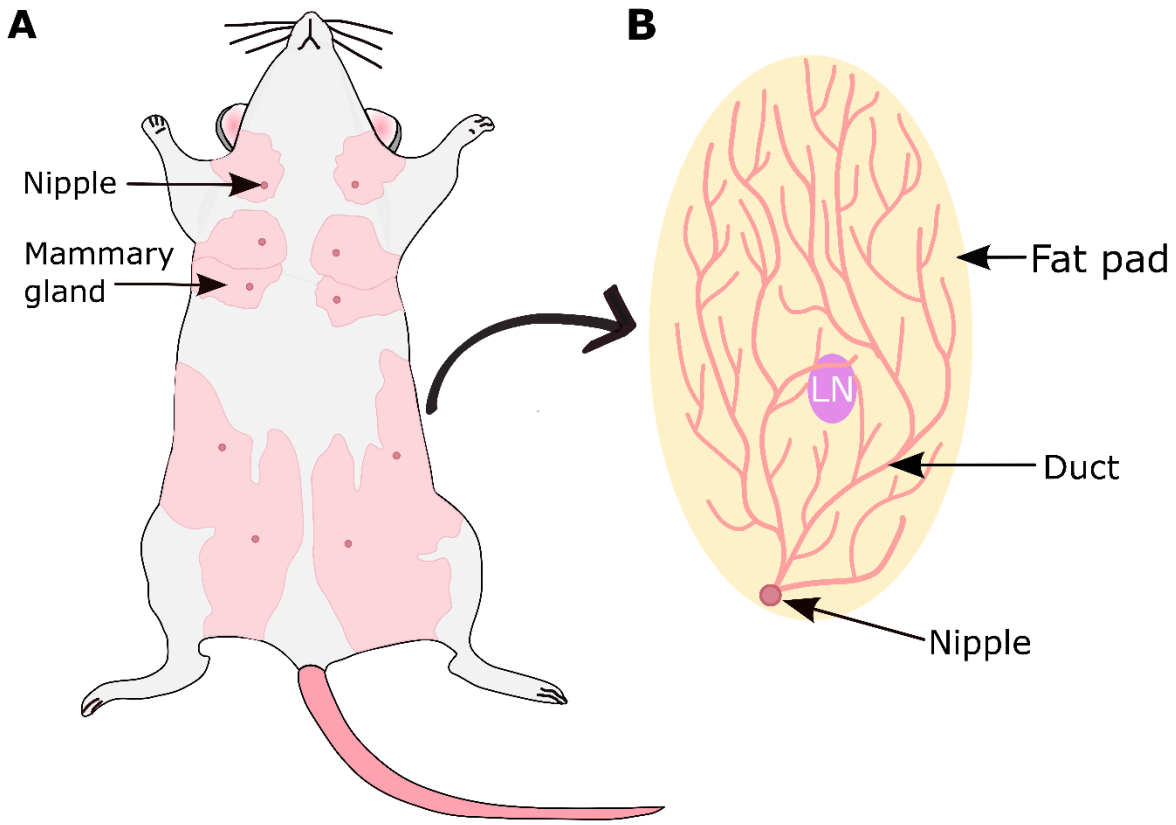


**Figure 2: Overview of mouse mammary gland structure.** (A) Mice have five pairs of mammary glands. (B) The mature virgin mouse mammary gland represents a ductal tree that is embedded in a fat. The abdominal mammary gland represented in the figure is also accompanied by a lymph node (LN).

## 1.2 Mammary gland cell types and their function

### 1.2.1 Mammary basal epithelial cells

The mature resting mammary gland alveolar ductal wall is made up of an epithelial bilayer, where the inner luminal cell layer is surrounded by the basal cell layer (Figure 1C). The basal layer consists of contractile myoepithelial cells and putative mammary stem cells, which are in contact with the basement membrane (Macias & Hinck, 2012). Importantly to mammary gland development, also some of the luminal cells are in contact with the basement membrane, which is of importance to cell differentiation (Englund et al., 2021).

The basal cells have smooth muscle cell –like properties, such as the ability to contract (Adriance et al., 2005). Accordingly, they express contractile smooth muscle-like proteins, like smooth muscle actin (SMA) and smooth muscle myosin heavy chain (Gieniec & Davis, 2022), which are required for the cells' contractile function and successful lactation (Haaksma et al., 2011; Weymouth et al., 2012). In the functionally matured mammary gland basal epithelial cell contraction is initiated trough

the receptor binding of oxytocin hormone, which is released from the posterior pituitary to maternal circulation in response to neonate suckling (Gieniec & Davis, 2022; Gimpl & Fahrenholz, 2001). On cellular level, the activation of oxytocin receptor sets of a signalling cascade resulting in increased intracellular $Ca^{2+}$ levels and formation of $Ca^{2+}$/calmodulin complex, which triggers the activation of myosin light-chain kinase (MLCK) (Gimpl & Fahrenholz, 2001; Olins & Bremel, 1982; Stevenson et al., 2020). MLCK phosphorylates myosin light-chain (MLC) changing its conformation, which enables the interaction of myosin with actin (Vasquez & Martin, 2016; Webb, 2003). Moreover, the myosin adenosine 5'-triphosphatase (ATPase) is activated releasing adenosine-5'-triphosphate energy for myosin movement along the actin filaments, which generates contraction (Vasquez & Martin, 2016; Vicente-Manzanares et al., 2009). Also Rho-associated protein kinase (ROCK), coiled-coil kinase and citron kinase have a role in the contraction initiating pathway (Vasquez & Martin, 2016). Nonetheless, it has been recently suggested that there might be other possible pathways that initiate mammary basal epithelial cell contraction, when the pathway described above is altered or obstructed (Stevenson et al., 2020). Stevenson et al. (2020) showed that the lactating mammary gland was able to contract even when the contractile pathway was pharmacologically inhibited, which indicates that mammary gland contraction is a highly complex process.

The simultaneous contraction of the alveoli surrounding basal cells results in milk ejection from the alveolar lumen trough the mammary ductal system all the way to the nipple (Adriance et al., 2005; Tortora & Bryan, 2014). Moreover, the contraction of the basal epithelial cells has also been suggested to aid the milk lipid droplet secretion from the milk producing luminal epithelial cells by mechanical constriction (Mather et al., 2019). Although cellular contractility of non-muscle cells has been studied, many questions remain to be answered regarding the milk ejection mechanism, such as cellular force generation and signal transduction (Gieniec & Davis, 2022). Furthermore, several cellular components are suspected to aid cell contraction, but their role is not fully characterised (Adriance et al., 2005; Gieniec & Davis, 2022). For example integrins, a type of cellular adhesion and signalling receptors, have been proposed to be essential in enabling mammary epithelial cell contraction (Paavolainen & Peuhu, 2021; Raymond et al., 2011). Integrins connect the actin cytoskeleton to the extracellular matrix (ECM), and mediate signals, which modulate the cell contractility (Huveneers & Danen, 2009).

In addition to contraction during nursing, the basal epithelial cells provide structural support for the mammary gland. Relevantly, basal epithelial cells are thought to have a barrier role in tumour metastasis. That is, basal cells hinder malignant luminal cells growth and invasion into the surrounding stroma. Moreover, basal cells are theorised to possess resistance to malignant

transformation and the loss of basal epithelial cell function is associated with cancer invasiveness and metastasis. (Adriance et al., 2005)

Novel research methods, like single-cell ribonucleic acid (RNA) sequencings of mouse mammary glands, have also revealed that mammary basal epithelial cells are heterogenic (Bach et al., 2017). Briefly, the mammary basal epithelial compartment includes basal cells with high oxytocin receptor expression and contractile potential, and basal cells, which are thought to have a particular regenerative capacity (Bach et al., 2017). Moreover, it has been observed that basal epithelial cells in adult mice can reactive bipotency upon injury of luminal compartments (Centonze et al., 2020), which further suggests that mammary epithelial cells are incredibly peculiar and adaptive. Nonetheless, there is uncertainty whether all smooth muscle-like proteins expressing cells in the basal compartment are able to contract (Gieniec & Davis, 2022), and therefore smooth muscle-like mammary epithelial cells will be referred to as basal epithelial cells rather than myoepithelial cells in this thesis.

### 1.2.2 Mammary luminal epithelial cells

Similarly to the basal compartment, the luminal compartment in the mammary epithelium consists of a heterogenous population of cells. Luminal cells are especially distinguished from each other based on the expression of oestrogen receptor, which is thought to be expressed by about half of the mature luminal cells, which of most also express progesterone receptors (Arendt & Kuperwasser, 2015). Furthermore, Shehata et al. (2012) proposed that there are progenitor cells with different levels differentiation capacities in the luminal compartment (Shehata et al., 2012). However, there is still some controversy about the putative luminal progenitor cells and their properties (Cristea & Polyak, 2018). For example, luminal progenitor cells are suggested to be hormone insensitive and relying on paracrine signalling upon mammary gland differentiation (Inman et al., 2015), while it has also been proposed that some luminal progenitor cells express oestrogen receptors (Shehata et al., 2012; Watson, 2021). Nevertheless, it is thought that these progenitor cells have a high proliferative capacity and have an important role in alveolar differentiation during lactation (Watson, 2021).

During pregnancy the epithelial cells in the luminal compartment differentiate into milk-producing cells, commonly also termed lactocytes (Hassiotou & Geddes, 2013). The milk-producing cells synthesise milk lipid droplets, which are essential components of the maternal milk for neonate nourishment (Hassiotou & Geddes, 2013; Mather et al., 2019). Milk lipid droplets are synthesised in the rough endoplasmic reticulum, where triglyceride-rich lipid core is surrounded by a monolayer composed of phospholipids and various proteins (Mather et al., 2019). During the transit from endoplasmic reticulum to the apical site of the cell, where from they are ultimately secreted to the

alveolar lumen, lipid droplets fuse together and grow in size (Masedunskas et al., 2017; Monks et al., 2020). The final lipid droplet diameter ranges from less than 200 nm to over 15 μm across different species (Mather et al., 2019). Upon secretion the lipid droplets further expand and gain an additional outer membrane bilayer from the cell plasma membrane (Masedunskas et al., 2017; Mather et al., 2019). The exact mechanism of the lipid droplet release from milk-producing luminal epithelial cells is unclear, but it is known that the oxytocin-induced contraction of basal epithelial cells contributes notably to the secretion, and that the milk lipid droplet size does not affect the secretion capability (Masedunskas et al., 2017; Mather et al., 2019; Monks et al., 2020).

Nevertheless, in addition to basal epithelial cell contraction, it has also been suggested that milk secreting luminal cells might move themselves further aiding the release of the milk lipid droplets to the alveolar lumen (Mather et al., 2019; Mroue et al., 2015). The $Ca^{2+}$ released from the intracellular stores of basal cells are thought to proceed through gap junctions to luminal cells, where the increased $Ca^{2+}$ concentration initiates actin cytoskeletal contraction at the apical surface and thus causes the release of milk droplets (Mroue et al., 2015). Taken together, milk production and secretion are complex processes, that require further investigation.

### 1.2.3 Other cell types of mammary gland

There is some ambiguity in the definition of mammary stem cells, but it is apparent that the mammary gland contains cells that are able to regenerate and drive the mammary gland development and robust differentiation. Moreover, there are various progenitor cell types that give raise to particular structures during different developmental stages, and it is plausible that there are various stem and progenitor compartments present in the different developmental stages of the mammary gland. However, lack of exclusive markers for putative mammary stem cells and progenitor cells complicates precise definition of the cells (Watson, 2021)

In addition, various other cell types, such as fibroblast, adipocytes and immune cells, within the breast contribute to mammary gland development and function. Stromal fibroblasts synthesise, for example, growth factors, cytokines and ECM components that aid and guide mammary gland development (Inman et al., 2015). Adipocytes in turn are abundant in the non-lactating breast and support mammary gland structure (Inman et al., 2015). Importantly, adipocytes provide lipids and metabolites for mammary gland growth and lactation, but they also have a role in mammary cross-talk and communication trough paracrine and endocrine signalling (Hovey & Aimo, 2010). Altogether, different cells within the breast cooperate extensively to initially enable nursing.

## 1.3 Mammary gland development

Unlike in many other organs, a major part of mammary gland development takes place after birth, and it becomes fully functional first during pregnancy and lactation. Mammary gland development begins during embryogenesis and continues gradually through the prenatal life resulting in mammary anlage (Figure 3, birth) (Macias & Hinck, 2012). After birth the mammary gland undergoes minimal growth (Hassiotou & Geddes, 2013). During the pubertal expansion, however, the mammary gland grows remarkably, and the ductal three elongates and branches in response to increased levels of, most importantly, ovarian oestrogen, growth hormone from pituitary gland, and various growth factors, like insulin-like growth factor (Inman et al., 2015; Macias & Hinck, 2012). Moreover, progesterone has a necessary role in mammary gland branching (Atwood et al., 2000; Lydon et al., 1995).

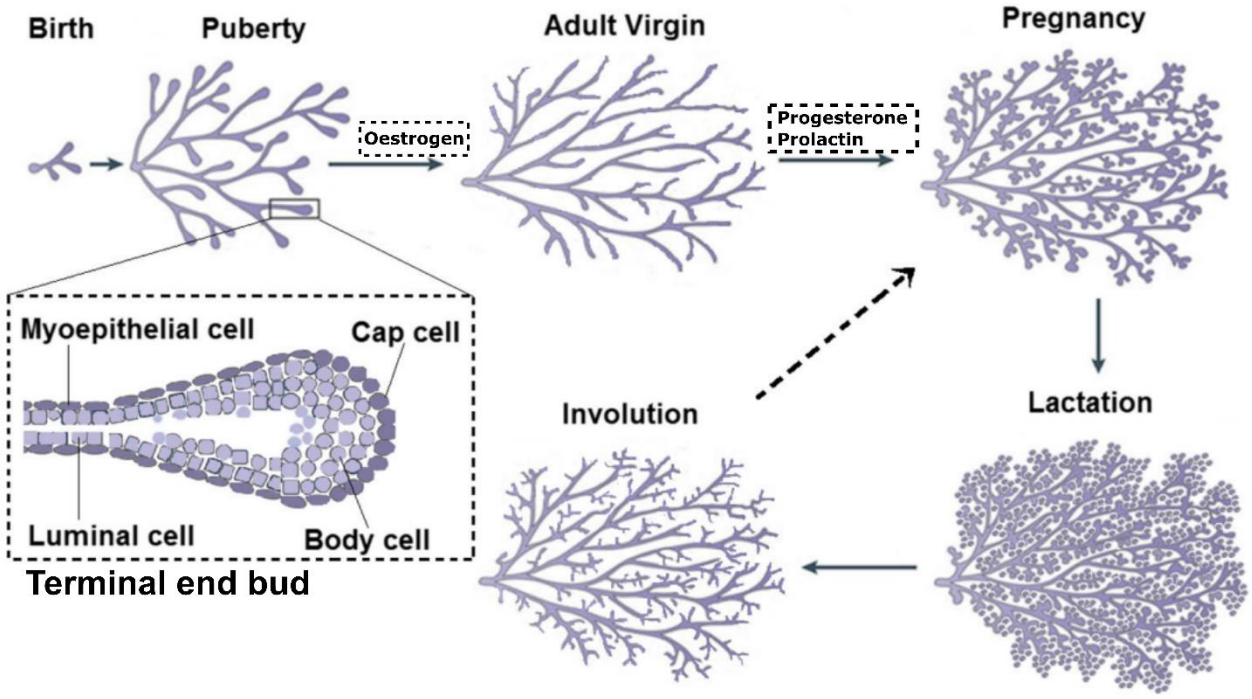


**Figure 3: Mammary gland development**. At birth, mammary gland represents a mammary gland anlage. During puberty the mammary gland grows extensively resulting in a mammary tree mainly in response to oestrogen hormone, but also growth hormone and growth factors. Pubertal differentiation gives rise to terminal end buds (TEB), that direct the duct elongation. In response to increased levels of progesterone and prolactin, among others, the mammary gland branches further and undergoes lobulo-alveolar differentiation to prepare itself for lactation. In absence of breast feeding the mammary gland undergoes involution. Image modified from Paine and Lewis 2017 (Reproduced by the permission of CC-BY license).

Puberty gives rise to terminal end buds (TEB) (Figure 3), bulb shaped structures in the end of the ducts, that direct the duct elongation and branching into mammary fat bad (McNally & Stein, 2017;

Paine & Lewis, 2017). The TEB consist of two distinguishable compartments: a single layer of "cap cells" at the front and the inner "body cells" layer. The cap cells mainly differentiate to basal cell precursors, and body cells to luminal cells and include alveolar progenitors (McNally & Stein, 2017; Paine & Lewis, 2017). The cap and body cells at the foremost tip are less differentiated, and the cap cell compartment is even suggested to contain multipotent mammary stem cells, while the narrow part following the tip contains more differentiated cells (Paine & Lewis, 2017). Eventually, TEBs regress when they reaches the end of the fat pad leaving behind an extensive mammary tree (Figure 3, adult virgin)(McNally & Stein, 2017). The formation of mammary tree is carefully coordinated, and the branching level is regulated so that there is sufficient space for alveolar differentiation that occurs during pregnancy (McNally & Stein, 2017). Branching morphogenesis is substantially coordinated by the surrounding ECM and stromal cells (Schedin & Keely, 2011). In fact, the mammary epithelial cells communicate actively with each other and a large variety of other stromal cell types and ECM cues during all phases of mammary gland development (Inman et al., 2015). For example, the ECM guide cellular behaviour, such as proliferation, differentiation and organisation, through cellular adhesion molecules (Paavolainen & Peuhu, 2021; Sternlicht, 2005). In addition, the immune cells navigate invasion of mammary branches into the fat bad and clear apoptotic epithelial cells, among other things (Gouon-Evans et al., 2000; Inman et al., 2015).

During the menstrual cycle (oestrus cycle in rodents) the mammary gland further branches from the previously established mammary tree (Geddes, 2007; Paine & Lewis, 2017). The cycle can be divided to follicular and luteal phases, where the follicular phase is characterised by peak in the circulating oestrogen, and the luteal phase by increased level of progesterone (Arendt & Kuperwasser, 2015; Slepicka et al., 2021). The increased progesterone level has been found to be essential in stimulating the mammary gland tertiary side-branching during the cycle (Brisken et al., 1998; Sternlicht, 2005). However, some of this progesterone induced mammary gland proliferation also regress over the course of menstrual cycle (Geddes, 2007).

Upon pregnancy the mammary gland starts rapidly differentiating in response to the increased levels of circulating prolactin and progesterone, among other actors. Progesterone production is maintained by corpus luteum during the early pregnancy and produced later by the mature placenta (Vannuccini et al., 2016), and prolactin is secreted from the pituitary gland in response to elevated progesterone levels, among others (Freeman et al., 2000). Like in pubertal development, also here progesterone has an essential role in side-branching (Macias & Hinck, 2012). The secondary and tertiary ductal side-branching is rapid and extensive during the early pregnancy, and establishes a base for the lobulo-alveolar differentiation (Macias & Hinck, 2012). At the tertiary branch tip, progesterone

together with prolactin initiates the formation of alveolar buds which are eventually cleaved and differentiated into distinct alveoli later during the pregnancy (Figure 3, pregnancy) (McNally & Stein, 2017; Richert et al., 2000). The differentiated alveolus is comprised of secretory luminal epithelial cells surrounded by a discontinuous layer of contractile basal epithelial cells allowing direct contact between luminal epithelial cells and the underlying basement membrane (Figure 4) (Gieniec & Davis, 2022; Macias & Hinck, 2012; Oakes et al., 2006). The direct contact between luminal epithelial cells and basement membrane is theorised to be necessary for the mammary gland differentiation (Macias & Hinck, 2012; Paavolainen & Peuhu, 2021). Even though mammary epithelial cells largely fill up the breast volume (Figure 3, lactation), also mammary gland adipocytes expand and display increased metabolic activity during pregnancy and lactation (Hovey & Aimo, 2010). Moreover, the mammary gland ECM is remodelled during pregnancy in response to hormonal changes and signalling along with the epithelium, which prepares it for its' role in regulating the mammary epithelium during differentiation (Inman et al., 2015).

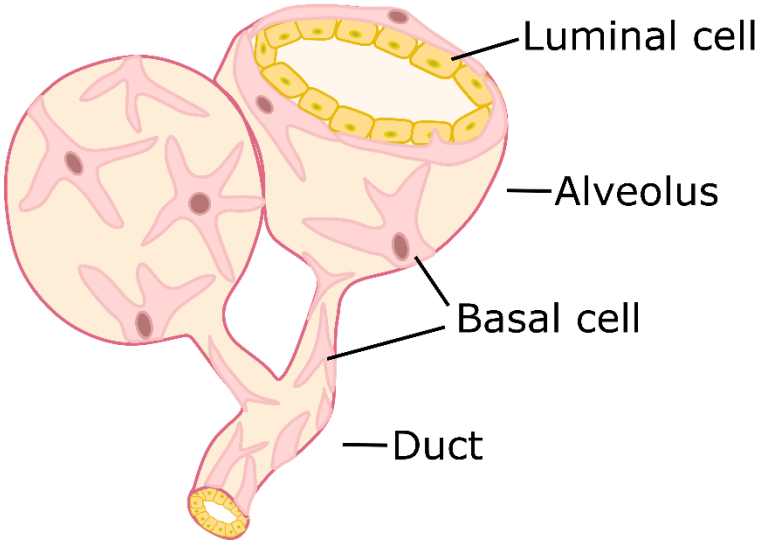


**Figure 4: Lactating mouse mammary gland alveolus.** Image adapted from Gieniec & Davis 2022.

Parturition and delivery of the placenta leads to rapid decrease in systemic progesterone levels, which together with increased prolactin production leads to notable up-regulation of milk synthesis (Hassiotou & Geddes, 2013). Now the mammary gland is ready for nursing. During the course of lactation the hormone prolactin is continued to be secreted in response to neonate suckling, which maintains the functional structure of mammary gland until milk stasis (McNally & Stein, 2017). The decrease of prolactin levels signals the mammary gland to undergo involution (Figure 3, involution) (McNally & Stein, 2017). During involution, the milk-producing compartments undergo carefully controlled apoptosis resulting in the collapse of the alveoli (Radisky & Hartmann, 2009). Moreover,

parts of the basement membrane and ECM are broken down during the later phases of involution, which induces an excessive tissue remodelling and further cell deaths (Macias & Hinck, 2012; McNally & Stein, 2017). Eventually, the mammary glands revert to the mature resting state. Nonetheless, the mammary gland has a remarkable regenerative ability and can differentiate and become fully functional to lactate again. This ability has been attributed to luminal and basal epithelial progenitor cells (Watson, 2021).

## 1.4 Vimentin

Vimentin is an intermediate filament (IF) protein found in many different cell types of mainly mesenchymal origin (Alberts et al., 2015). IFs together with microfilaments and microtubules form the cell cytoskeleton, which is an intracellular protein framework that provide support and strength for the cell (Alberts et al., 2015; Fletcher & Mullins, 2010). IF proteins, including vimentin, have a strong rope-like structure and they are the most flexible of the cytoskeletal proteins (Alberts et al., 2015; Ostrowska-Podhorodecka & McCulloch, 2021). Vimentin is composed of helical polypeptides that together shape a coiled-coil dimer (Danielsson et al., 2018; Kraxner et al., 2021). Two dimers form tetramers, and several tetramers together can, in turn, form a unit-length filament (ULF)(Kraxner et al., 2021). The ULFs associate further to each other, finally assembling to a larger flexible filament (Pérez-Sala et al., 2015).

Typically, vimentin protein filaments form a network that is organized around the nucleus, from where it stretches through the cytoplasm providing mechanical strength to the cell (Danielsson et al., 2018) (Figure 5). Around the nucleus, vimentin filaments form a cage-like structure that encapsules it, which is thought to protect the nucleus from deoxyribonucleic acid (DNA) damage and maintain its' shape (Ostrowska-Podhorodecka et al., 2022; Patteson, Vahabikashi, et al., 2019). Via various crosslinkers, such as plectin, vimentin can be crosslinked to other cytoskeletal proteins, like microtubules and actin, and the formed network enables mechanotransduction from the cell surface to the nucleus and thus allows the cell to detect mechanical stress (Patteson et al., 2020). In addition, trough interaction with integrin receptors vimentin mediates information about ECM stiffness and stabilises adhesion between the cell and ECM (Ostrowska-Podhorodecka et al., 2021; Ostrowska-Podhorodecka & McCulloch, 2021). Moreover, vimentin is involved in anchoring cell organelles contributing to maintenance of polarity (Danielsson et al., 2018). Importantly, the vimentin cytoskeleton is not a rigid and passive structure, but possess certain flexibility and tensile memory, that allows modification of cell's mechanical properties (Danielsson et al., 2018; Ostrowska-

Podhorodecka et al., 2022). Altogether, the elasticity of vimentin is involved in various cellular functions.

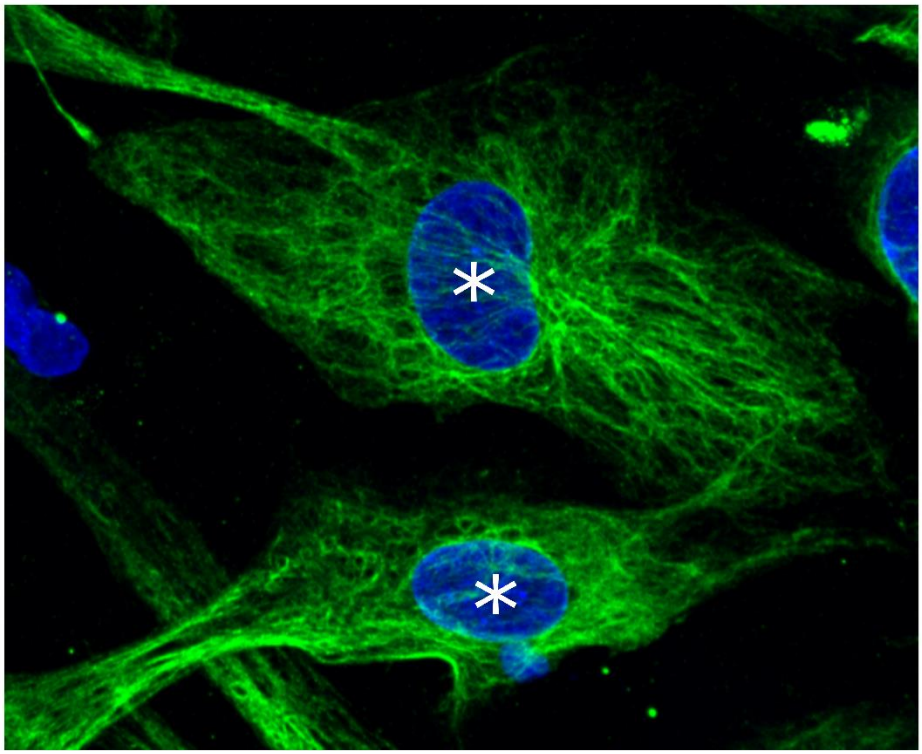

**Figure 5: Cellular location of vimentin intermediate filaments (green).** Location of nuclei (blue) indicated with stars**.** Image by Emilia Peuhu.

Vimentin also has a prominent role in many physiological processes, such as cell differentiation, adhesion and movement (Danielsson et al., 2018). In addition, there is a particular interest in vimentin's role in cell migration and invasion, since they are not only related to normal physiological functions but also to the spreading of cancer. Vimentin has been shown to have several functions in promoting migration (Battaglia et al., 2018). For example, vimentin filaments maintain cell polarity trough association with rearranging microtubules during directed migration and coordinate actin dynamics by regulating actin retrograde flow (Battaglia et al., 2018; Gan et al., 2016; Jiu et al., 2015). In addition, vimentin has an important role in maintaining cellular shape and resisting mechanical stress during migration (Ostrowska-Podhorodecka et al., 2022). Patteson et al. (2019) demonstrated the mechanical properties of vimentin by showing that vimentin provides a protective cage around the nucleus, which prevents nuclear rupture and promotes cell stability (Patteson, Vahabikashi, et al., 2019). Furthermore, vimentin has been under extensive research regarding in epithelial-mesenchymal transition (EMT), which is a process involved in, for example, development and tissue regeneration, but also cancer cell invasion, where it is often out of control (Liu et al., 2015). It is well established that vimentin is upregulated in EMT and promotes the cell motility, which is fundamental for cell

migration and invasion (Danielsson et al., 2018). The upregulation of vimentin upon EMT has also been reported to increase the metastatic potential of cancer cells, which is why vimentin is used as a clinical marker for malignant cell transformation and is also under interest as a drug target (Ridge et al., 2022; Strouhalova et al., 2020). Altogether, it is evident that vimentin is important in cellular stress response, regeneration, and motility.

Importantly, vimentin is involved in generating contractile forces in non-muscle cells through plectin-mediated crosslinking and regulating the assembly of actin stress fibres (Jiu et al., 2015, 2017). Vimentin has been suggested to negatively regulate the actomyosin contractility trough guanine exchange factor H1, which activates a small GTPase protein RhoA, which in turn promotes actomyosin bundle assembly and activates ROCK leading to MLC2 phosphorylation (Jiu et al., 2017). Moreover, it has been recently shown in mouse embryonic fibroblasts that vimentin filaments and actin directly interact with each other, and not just trough crosslinkers, and vimentin affects the actin-cytoskeleton contraction rate and magnitude (Wu et al., 2022). However, the role of vimentin in cell contractility is overall poorly understood and may vary in different cell types and environments (van Loosdregt et al., 2018). For example, Jiu et al. (2017) showed in human fibroblasts and osteosarcoma cells and that vimentin depletion leads to increased actomyosin contraction (Jiu et al., 2017). However, Liu et al. (2015) saw a decrease in contractile force generation upon vimentin depletion in breast cancer cells (Liu et al., 2015). Altogether, vimentin is involved in both generating contractile forces and providing cells with mechanical strength required for contraction, but the role of vimentin in generating contractile forces requires further investigation that would allow us to understand its impact in different cellular functions and physiological settings.

Despite the fact that vimentin has several important functions and wide distribution in different organs, the vimentin knock-out (*Vim*$^{-/-}$) mice are not lethal, and at first showed a rather undisturbed phenotype (Colucci-Guyon et al., 1994). However, later studies have identified a range of phenotypes associated with defects for example in vascular function, wound healing and lymphocyte migration (Danielsson et al., 2018). Overall, the vimentin knockout phenotypes typically manifest when the mice are challenged in one way or the other, further highlighting the role of vimentin in dampening cell stress.

In the mammary gland, vimentin is expressed in the basal cell layer and stromal cells. Previous examination by Peuhu et al. (2017) showed that vimentin is involved in the ductal outgrowth during mammary gland development. Moreover, vimentin deficiency led to reduced proportion of basal epithelial cells in mammary ducts and enlarged mammary epithelial lumen in mice (Figure 6).

However, the pregnancy and lactation related differentiation of the mammary gland was not macroscopically disturbed, and *Vim*$^{-/-}$ mice could still nurse their offspring. Nonetheless, the knowledge about the role of vimentin in mammary gland function was sparse and required further investigation. (Peuhu et al., 2017)

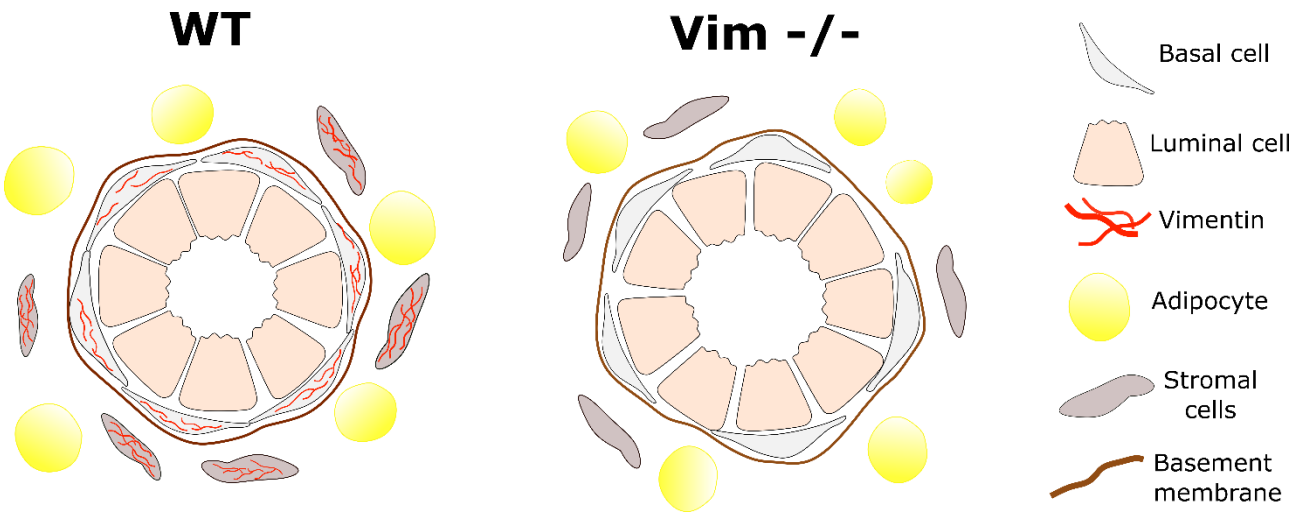


**Figure 6: Schematic illustration of the function of vimentin in mouse mammary gland duct.** Vimentin deficiency reduces basal epithelial cell number. Image adapted from Peuhu et al. 2017.

# 2 Aims of the research project

Based on previous literature, vimentin IF protein has a notable role in many cell types and tissues. However, as summarised in the introduction, its contribution to normal mammary gland function remains unclear. Since vimentin has been shown to be involved in both mammary gland development and cell contractility, investigation of its role in basal mammary epithelial cells may provide valuable insight in the regulation of mammary gland contractility, which is especially important during lactation, but also relevant to cell motility in the context of breast cancer. Thus, the goal of this research was to determine the role of vimentin in mammary gland morphogenesis and basal epithelial cell contraction during lactation.

The hypothesis of this project was that vimentin deficiency alters mammary epithelial differentiation during lactation and causes defects in basal epithelial cell contraction in mouse mammary gland. Furthermore, I hypothesised that vimentin downregulation disturbs basal epithelial cell contraction also in human mammary epithelium.

The first specific aim of this project was to investigate closer the mammary gland phenotype of the vimentin knockout (*Vim*$^{-/-}$) mice during lactation. Even though lactating *Vim*$^{-/-}$ mammary gland was not macroscopically disturbed (Peuhu et al., 2017), breeding of the *Vim*$^{-/-}$ mice has revealed challenges in consecutive pregnancies, and closer examination of the lactating gland showed potential differences in the alveolar structure. Therefore, detailed analysis of the histology of lactating *Vim*$^{-/-}$ mammary gland remained to be done.

It is plausible that changes in basal epithelial cell fraction and function might alter the ability of *Vim*$^{-/-}$ mice to lactate. Thus, the second specific aim was to assess the role of vimentin in basal epithelial cell contraction in human and mouse mammary gland.

# 3 Results

## 3.1 *Vim*$^{-/-}$ mice do not have obvious defects in nursing capabilities

The role of vimentin has been extensively studied in vimentin-deficient mice for nearly three decades and a wide range of physiological and pathophysiological phenotypes have been found (Danielsson et al., 2018; Ridge et al., 2022). Even though vimentin knockout mice were first reported to be able to reproduce without obvious phenotype (Colucci-Guyon et al., 1994), several laboratories have noted that the *Vim*$^{-/-}$ female mice have higher variation in breeding capacity. In other words, some *Vim*$^{-/-}$ dams produce normal number of pups and litters while others fail compared to wild type (WT) dams. Unpublished data from the laboratory suggested that *Vim*$^{-/-}$ dams produce fewer litters than WT, and the litters are somewhat smaller. To formally investigate the hypothesis that vimentin deficiency reduces the capacity of some mice to produce live offspring, the first litters of WT and *Vim*$^{-/-}$ female mice were investigated on the first day after birth. The litters of *Vim*$^{-/-}$ mice were somewhat smaller with the average litter size of 6.6 pups when compared to the WT litters that had an average of 9.3 pups per litter. Although some *Vim*$^{-/-}$ were indeed less capable of breeding (*Vim*$^{-/-}$ litter size ranged from 2-9 pups per litter and WT from 5-16 pups per litter), there was no statistically significant difference in the size of litters investigated during this study (Figure 7A) ($p=0.0837$, two sample t-test). Importantly, all WT and *Vim*$^{-/-}$ one-day-old pups were observed to have milk in their stomach (Figure 7B), and all the pups of the first litters of WT and *Vim*$^{-/-}$ dams were alive at the time of weaning (Figure 7C), which demonstrates that vimentin does not abrogate nursing and the *Vim*$^{-/-}$ dams are capable of feeding their offspring. Moreover, no obvious anomalies were observed in the offspring.

To follow up the weight gain in WT and *Vim*$^{-/-}$ pups during nursing, entire litters were weighed weekly until weaning. Preliminary data regarding the body weight of pups during the course of lactation suggests that WT or heterozygous pups that were born to *Vim*$^{-/-}$ dams gained weight at similar pace as pups born to WT dams (Figure 7D). Overall, the data demonstrate that *Vim*$^{-/-}$ mice do not have obvious defects in nursing. However, the data also support the hypothesis that some *Vim*$^{-/-}$ dams may have reduced litter size compared to WT dams (Figure 7A).

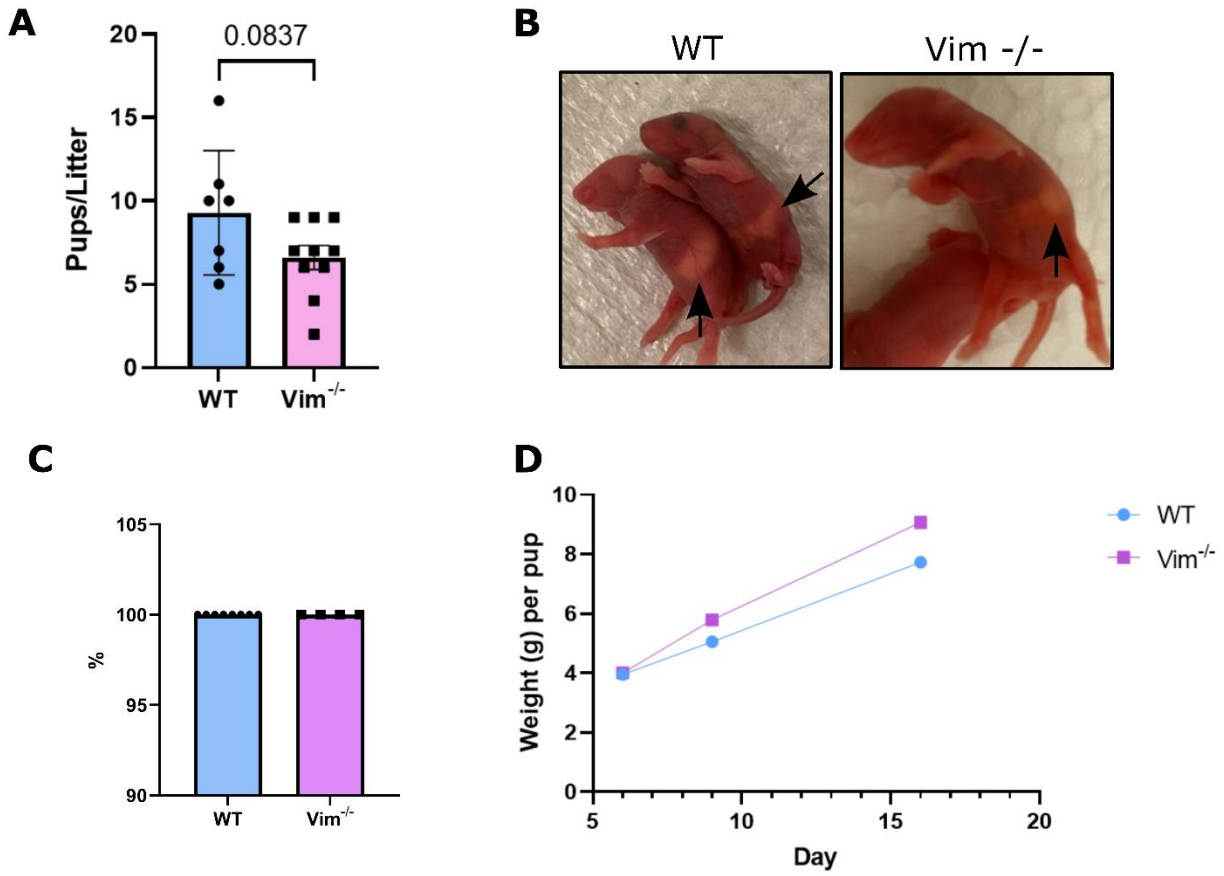


**Figure 7: Vimentin-deficient dams are able to breed and lactate.** (A) The first litters of vimentin knockout (Vim$^{-/-}$) dams were somewhat smaller than the wild-type (WT) litters, but the difference was not statistically significant (p=0.0837, two sample t-test) ($n_{wt}$=7 litters, $n_{Vim}$-/-= 10 litters). Graph data shown as mean ± SEM. (B) The pups' white milk spots (arrows) indicate that the offspring has been fed ($n_{wt}$=4 litters, $n_{Vim}$-/-= 6 litters). (C) Proportion of the born pups still alive at weaning: all the pups of the first litters of WT and Vim$^{-/-}$ dams were alive at the time of weaning ($n_{wt}$=8 litters, $n_{Vim}$-/-= 4 litters). (D) The weight gain of WT and heterozygous litters born to either a WT or Vim$^{-/-}$ dam was followed during the course of lactation ($n_{wt}$=1 litter, $n_{Vim}$-/-= 1 litter). The preliminary results indicate that the pups gain weight at similar base. The graph shows the phenotype of the dams and the pup's average weight in each litter.

## 3.2 Vimentin deficiency alters the morphology of the lactating mammary gland

To detect possible defects in lactogenic differentiation of the mammary gland, that could be linked to reduced breeding capacity in some *Vim*$^{-/-}$ dams, the mammary gland phenotype of the *Vim*$^{-/-}$ and WT mice was investigate on the first day of lactation (i.e., the morning after birth; L1). Vimentin deficiency had previously been shown to reduce the number of basal epithelial cells and slow down ductal outgrowth during pubertal mammary gland development (Peuhu et al., 2017), but the role of vimentin in the lactating mammary gland has not been addressed in detail. Therefore, the mice mammary gland phenotype was first inspected on a macroscopical level using carmine alum stained mammary gland wholemounts. Both non-lactating and lactating *Vim*$^{-/-}$ abdominal mammary glands

had rather undisturbed morphology as compared to the WT mammary glands (Figure 8A, B). The whole mounts of 9-week-old virgin mammary glands showed an extensive ductal tree in both genotypes. The oestrus cycle phase affects the branching of the non-lactating mammary gland (Cole, 1933), and is likely to account for some variation in mammary gland branching level since the oestrus cycle was not normalized. As expected based on previous report (Peuhu et al., 2017) and the fact that *Vim*$^{-/-}$ mice are able to nurse their pups, vimentin deficiency did not impair pregnancy and lactation induced growth and differentiation of mammary gland (Figure 8B). On a macroscopic level the ductal branches had proliferated, and milk-producing alveoli had formed, which indicates that the *Vim*$^{-/-}$ mammary glands had undergone lobulo-alveologenesis to the same extend as the wild-type counterparts. Altogether, on a macroscopic level the *Vim*$^{-/-}$ abdominal mammary glands seem rather normal as compared to the WT mammary glands.

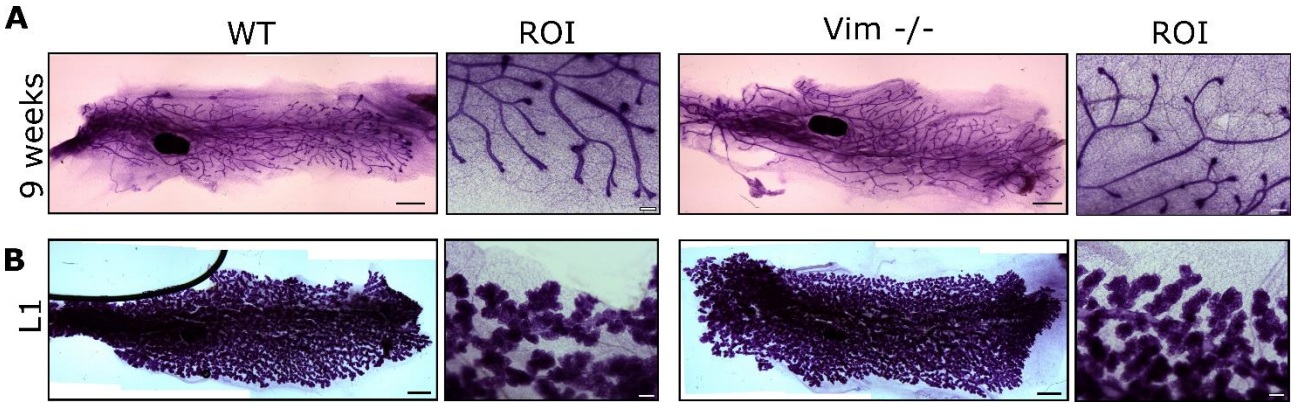


**Figure 8**: **Vimentin deficiency does not lead to obvious defects in mouse mammary glands at macroscopical level.** Mammary gland whole mounts of (A) 9-week-old virgin ($n_{wt}$= 3 mice, $n_{Vim-/-}$= 5 mice) and (B) first day lactating (L1) ($n_{wt}$=4 mice, $n_{Vim-/-}$= 6 mice) wild-type (WT) and vimentin knock-out (Vim -/-) mice and region of interest (ROI). Scale bars: 2 mm in whole mounts and 200 µm in region of interest (ROI).

Next, histological sections of L1 WT and *Vim*$^{-/-}$ mammary glands were investigated. Interestingly, the lumen of *Vim*$^{-/-}$ mammary gland alveoli appeared larger and the mammary gland morphology more diverse than in the WT mammary gland (Figure 9A). While the WT mammary glands formed organised and convergent lobular structures (Figure 9A, WT image 3), the *Vim*$^{-/-}$ mammary gland alveoli were generally more disorganised and irregular (Figure 9A, *Vim*$^{-/-}$ image 4). In addition, a greater variation in alveolar size within sections could be seen in *Vim*$^{-/-}$ mammary glands (Figure 9A, *Vim*$^{-/-}$ image 2) than in WT (Figure 9A, WT image 1). There was also variation in how scattered the alveoli were in the mammary gland tissue: some tissue sections showed more compact lobular structures with little stroma, while other alveoli formed more sparse structures with lot adipose tissue and stroma in between. Moreover, the more dispersed alveoli had a grape-like morphology (Figure 9A, WT image 5 and *Vim*$^{-/-}$ image 6). Nonetheless, these mammary gland sections with sparsely

placed alveolar structures could simply be from the edge of the dissected tissue piece, since similar variation in organisation could be detected in both WT and *Vim*$^{-/-}$ mammary glands (Figure 9A, WT image 5 and *Vim*$^{-/-}$ image 6).

However, more extensive image analysis of haematoxylin and eosin (H&E) stained mammary gland sections showed no statistically significant difference in the average alveoli lumen size between the genotypes (Figure 9B) (p=0.5926, unpaired t-test). Still, a larger variation in the alveolar size was observed for *Vim*$^{-/-}$ mammary glands (Figure 9C) (for multiple-comparison p-values of alveoli size per mouse see appendix 1). Here, segmented areas below 1000 μm$^2$ have been excluded as non-alveolar structures. The dams age at parturition ranged from 75 days to 201 days and number of pups from 4 to 11 (Table 1).

**Table 1: The age and number of pups of the investigated dams.**

| Mouse /dam | WT 72 | WT 73 | WT 1 | WT 2 | KO 44 | KO 54 | KO 55 | KO 56 | KO 57 | KO 61 |
|---|---|---|---|---|---|---|---|---|---|---|
| Age at parturition (d) | 75 | 76 | 89 | 90 | 159 | 76 | 75 | 75 | 76 | 201 |
| Number of pups | 10 | 6 | 5 | 7 | 11* | 7 | 9 | 6 | 9 | 4 |

*Eleven pups in a cage of two female mice, which of only one was undoubtedly at lactation stage.

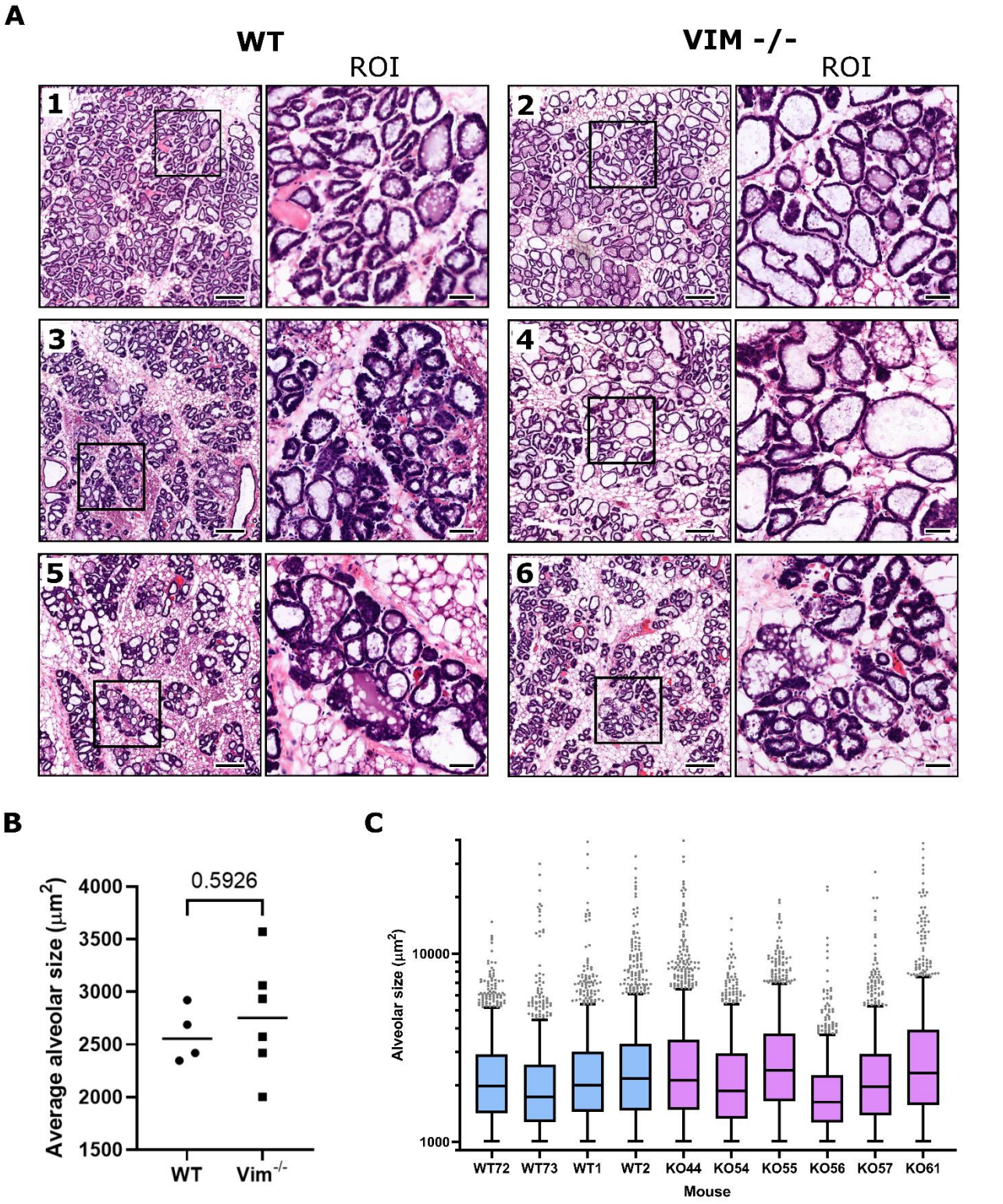


**Figure 9: Vimentin deficiency leads to disorganized morphology and variation in alveolar size.** (A) Haematoxylin and eosin stained mammary glands from lactating (day 1; L1) wild-type (WT) and vimentin knockout (Vim -/-) mice, and magnification of the region of interest (ROI). Scale bar: 200 µm and 50 µm in ROI. Alveolar size of L1 mammary glands was quantified using morphological segmentation in ImageJ: (B) average alveolar size (p=0.5926) and (C) Tukey's-boxplot of alveolar size per mouse. For age at parturition and number of pups of each dam see Table 1. Results from $n_{wt}$=4 mice, $n_{Vim-/-}$= 6 mice. The graphs represent alveoli larger than 1000 µm$^2$.

Immunohistochemical staining of the L1 mammary glands was done to visualise the localisation of vimentin in the lactating mammary gland. In the WT mammary glands vimentin was strongly expressed in stromal cells (Figure 10, stars), but small levels of vimentin signal could also be detected in the alpha-smooth muscle actin (αSMA)-positive basal epithelial cells (Figure 10, arrows). Moreover, the luminal epithelial cells did not express vimentin. As expected, these observations support previous findings (Peuhu et al., 2017). In addition, no vimentin was expressed in the *Vim*$^{-/-}$ mammary glands as anticipated.

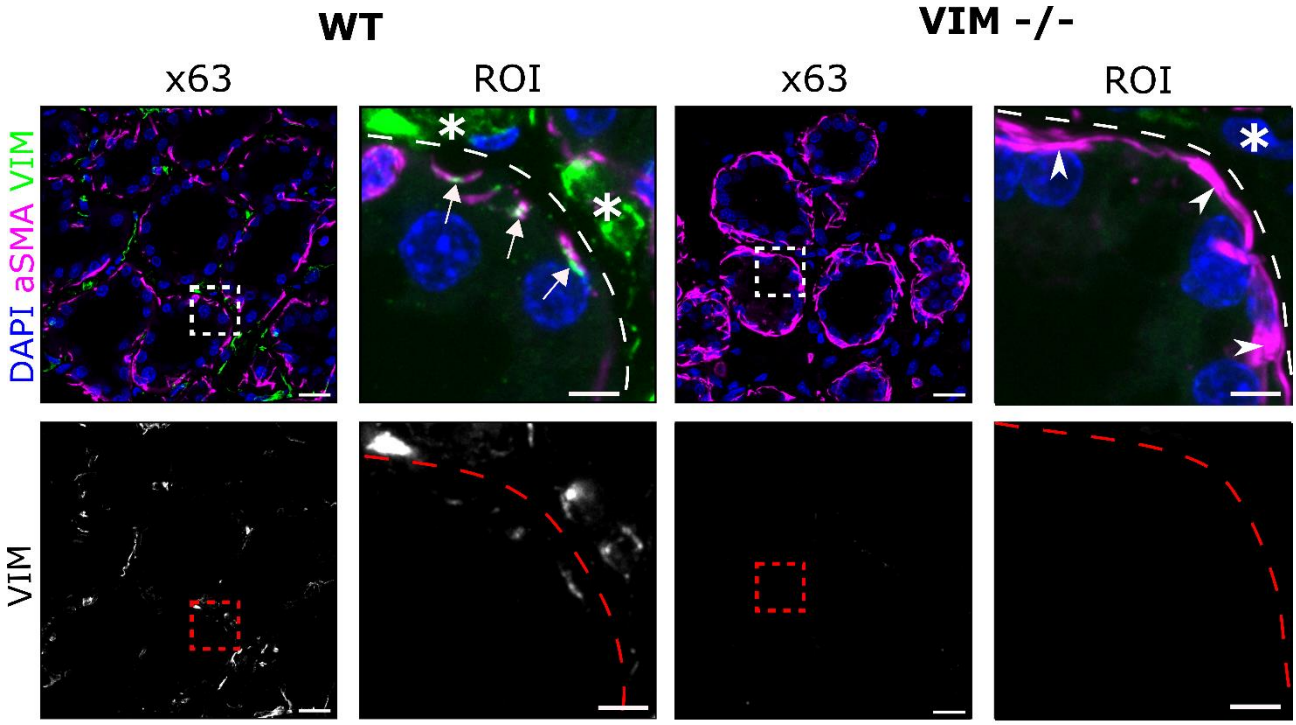


**Figure 10: Vimentin expression in lactating mouse mammary gland**. Vimentin (VIM), alpha-smooth muscle actin (α-SMA; basal cells) and DAPI (nuclei) stained L1 mammary glands ($n_{wt}$=2 mice, $n_{Vim-/-}$= 5 mice). Arrows indicate the vimentin positive basal epithelial cells, the arrow heads the vimentin negative basal epithelial cells, the stars the stromal cells and the dashed line the approximate position of alveoli basement membrane. Scale bars: 50 µm, and 10 µm in region of interest (ROI).

## 3.3 *Vim*$^{-/-}$ mammary epithelial cells have fewer but larger lipid droplets

To evaluate whether there are possible defects in milk secretion in vimentin-deficient mammary glands, the frozen sections of L1 mammary glands were stained using Nile red fluorescent stain (Figure 11A). Milk contains a large quantity of different lipids (German et al., 2002; Ragueneau, 1987), and thus staining of intracellular lipids with Nile red (Greenspan et al., 1985) can be utilised in visualising the milk lipid droplets of the lactating mammary gland. Moreover, filamentous actin

staining phalloidin was utilized for detecting the mammary gland epithelial cell morphology (Lengsfeld et al., 1974).

The image analysis of Nile red staining in the L1 mammary glands revealed that the *Vim*$^{-/-}$ mammary epithelial cells contain fewer but larger lipid droplets at first day of lactation compared to the WT cells (Figure 11B, C) ($p=0.0144$, two-sample t-test; $p=0.0025$, Mann-Whitney test, respectively). Since Nile red did not only stain intracellular lipid droplets, but clearly also the secreted lipids, the lipid droplet size and count in the alveolar lumen was assessed. Consistently, the average lipid droplet size was greater (Figure 11B), and the normalized droplet count smaller (Figure 11C) in the alveolar lumen of *Vim*$^{-/-}$ mammary gland, but the difference was not statistically significant ($p=0.3013$; $p=0.5815$, respectively, Mann-Whitney test). Moreover, the normalized total area of lipid droplets within the mammary gland epithelium was similar between WT and *Vim*$^{-/-}$ mammary glands ($p=0.3395$, two sample t-test), which suggests that vimentin deficiency does not affect the global lipid amount in the produced milk (Figure 11D). Interestingly, lipid droplets could also be detected outside the alveolar walls and the lumen (Figure 11A, arrows), which could be a result of milk leaking trough the epithelium.

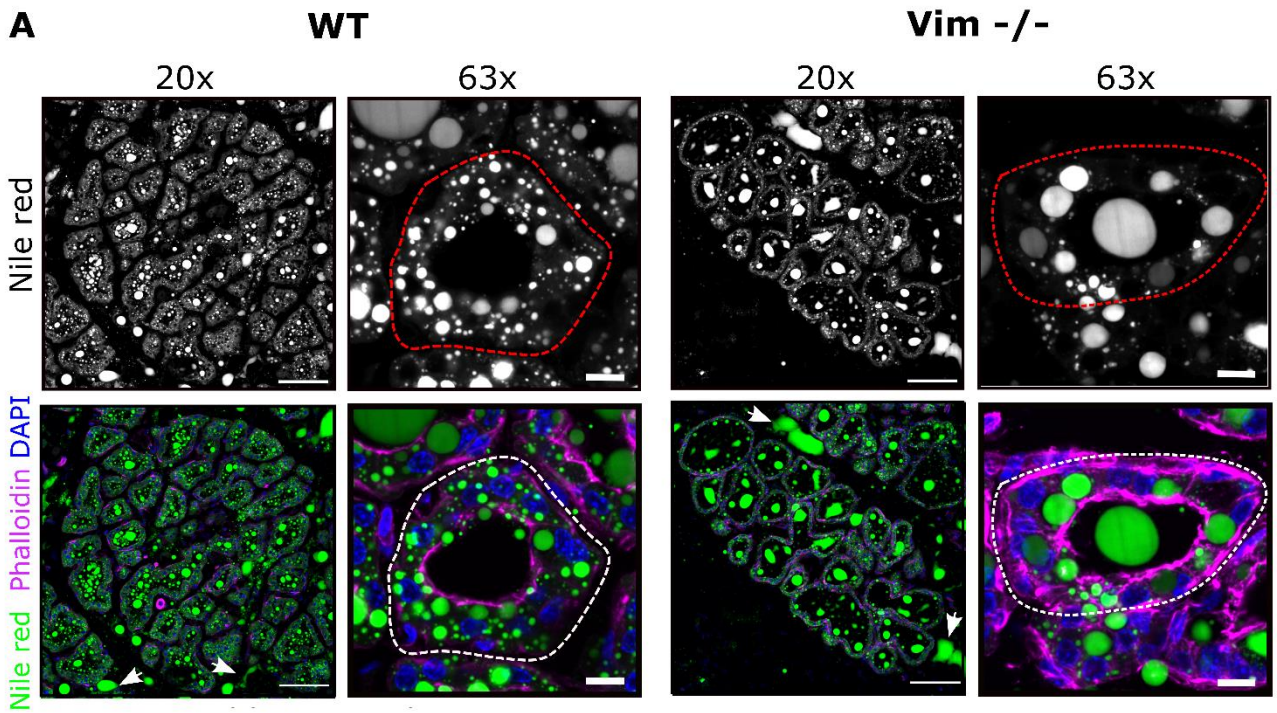
A
WT
Vim -/-
20x
63x
20x
63x
Nile red
Nile red Phalloidin DAPI

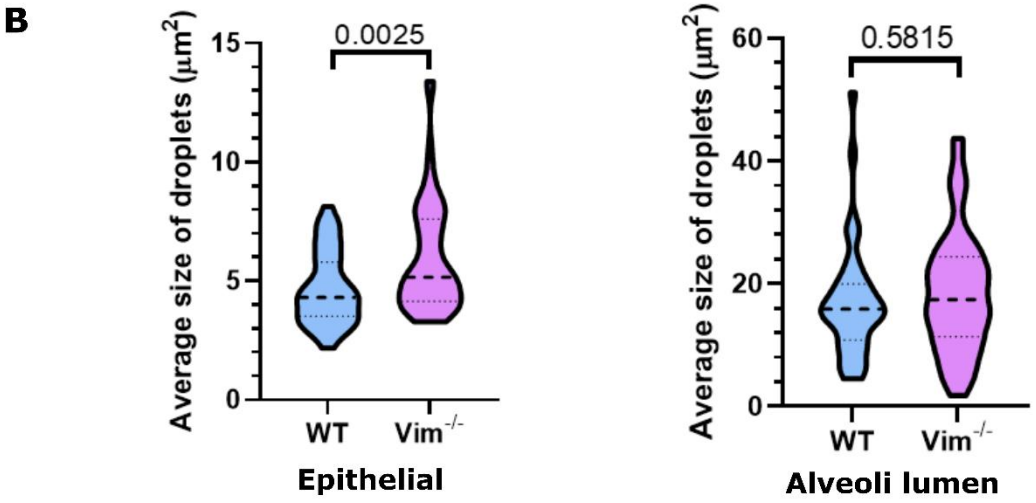
B
Average size of droplets (µm²)
0.0025
WT
Vim-/-
Epithelial
Average size of droplets (µm²)
0.5815
WT
Vim-/-
Alveoli lumen

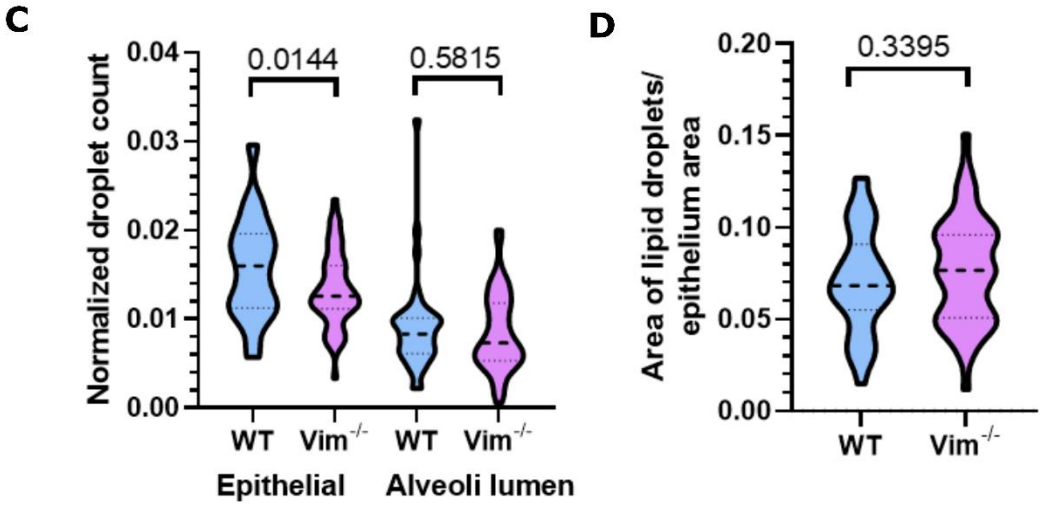
C
Normalized droplet count
0.0144
0.5815
WT
Vim-/-
WT
Vim-/-
Epithelial
Alveoli lumen
D
Area of lipid droplets/ epithelium area
0.3395
WT
Vim-/-

**Figure 11: Milk lipid droplet size and count in mouse mammary gland at first day of lactation** (A) Frozen sections of wild-type (WT) and vimentin knock-out (Vim-/-) mouse mammary glands at the first day of lactation (L1) stained for lipid droplets with Nile red, for filamentous actin with phalloidin and for nuclei with DAPI. The approximate position of alveoli is indicated with a dashed line, and the milk lipid droplets outside the mammary gland with arrowheads. Scale bars: in 20x magnification 100 µm and 63x magnification 10 µm. The size (B) and number (C) of lipid droplets within the WT and Vim-/- L1 mouse mammary gland epithelium and alveolar lumen was quantified in ImageJ. (D) The total area of lipid droplets within mammary gland epithelium was normalized by the area of mammary gland epithelium. Results from $n_{wt}$=4 mice and $n_{Vim-/-}$= 6 mice. Data presented as violin plots where dashed line represent the mean and thinner dashed lines the lower and upper quartiles.

## 3.4 Non-stimulated mouse mammary gland has little myosin phosphorylation

Myosin-light chain II (MLC2) is a component of non-muscle myosin II found in non-muscle cells, and its phosphorylation increases the cell contractility by increasing the ATPase activity of myosin (Vasquez & Martin, 2016). Immunohistochemical analysis of phosphorylated MLC2 (pMLC2) in lactating inguinal mammary glands has previously been utilized in investigating lactating mouse mammary basal epithelial cell contraction by Raymond et al. (2011).

In order to investigate basal epithelial cells' ability to contract in vimentin-deficient mammary gland, pMLC2 was labelled with a phosphorylation-site specific antibody in fixed frozen mouse mammary gland sections by IHC. The MLC2 was consistently phosphorylated in αSMA-positive basal epithelial cells of the 9-week-old virgin WT mammary gland (Figure 12A). However, upon labelling of L1 mammary glands of WT and *Vim*$^{-/-}$ mice we noted that specific pMLC2 labelling could not be detected in the basal epithelial cells of either genotype (Figure 12B). Since pMLC2 was successfully labelled in the non-lactating mammary gland stained during the same experiment, these results indicate that there is no detectable MLC2 phosphorylation in the basal epithelium of lactating mammary gland, and thus actomyosin contraction, at least without oxytocin stimulation. In the lactating mammary gland oxytocin rapidly activates the contraction initiating pathway and thus MLC2 phosphorylation, but pMLC2 is eventually also dephosphorylated (Gimpl & Fahrenholz, 2001; Olins & Bremel, 1982). Altogether, this readout could not be used for analysis of contractility in tissue sections of a lactating mammary gland.

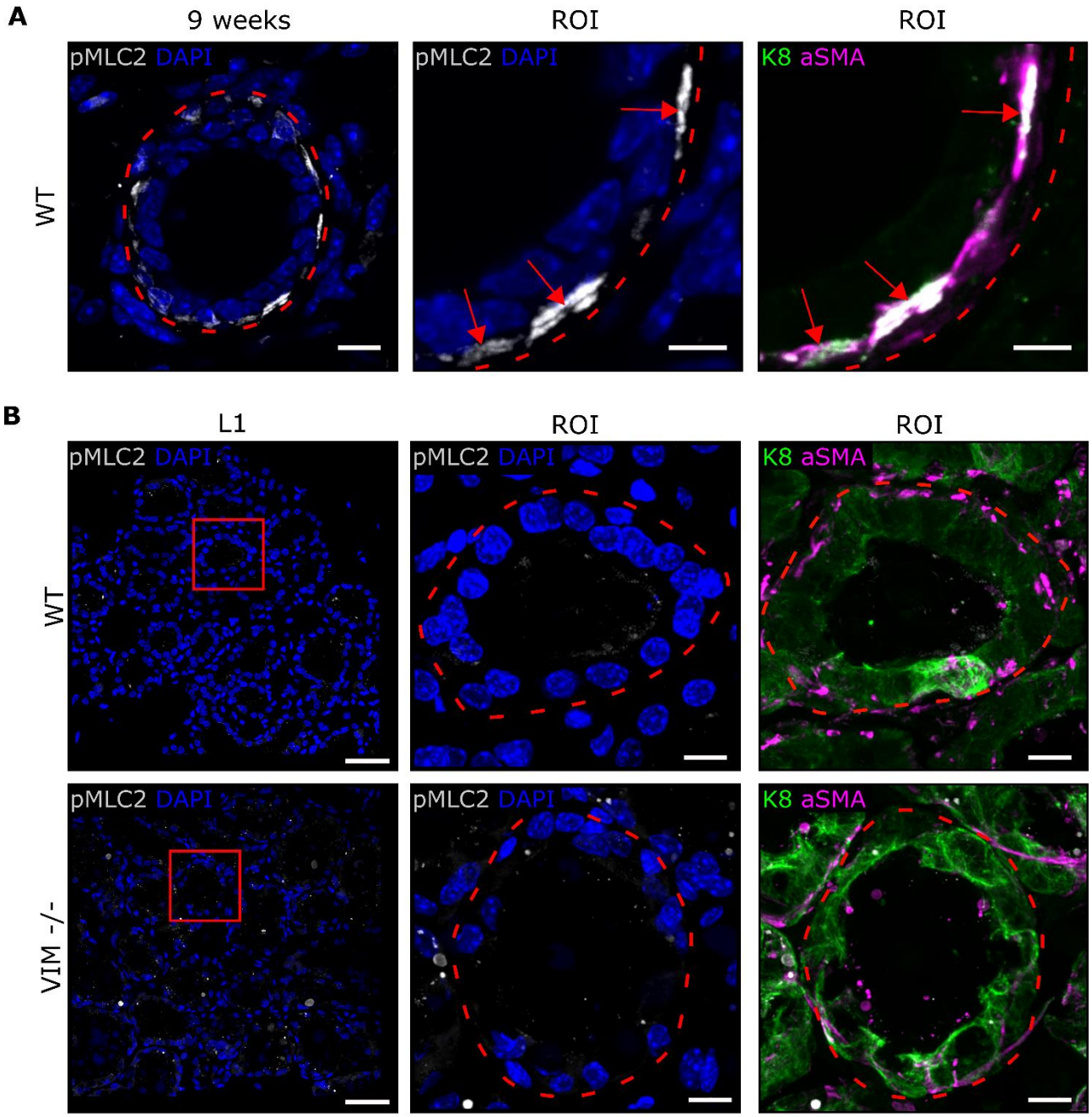


**Figure 12: Myosin light-chain 2 phosphorylation in mouse mammary gland.** Mammary gland frozen sections from (A) 9-week-old and ($n_{wt}$=1) (B) lactating (day 1; L1) ($n_{wt}$=4 mice and $n_{Vim-/-}$= 6) wild-type (WT) and vimentin knockout (*Vim*$^{-/-}$) mice were stained for phosphorylated myosin-light chain 2 (pMLC2, grey) and nuclei (DAPI; blue) (shown in left and middle column), and keratin 8 (K8, green) and alpha-smooth muscle actin (aSMA, magenta) (shown in right column). Scale bars: (A) 10 µm and 5 µm in region of interest (ROI), (B) 50 µm and 10 µm in ROI. Dashed line indicates approximate location of basement membrane and arrows on (A) panel the pMLC2 positive epithelial basal cells.

### 3.5 Myosin-light chain 2 phosphorylation does not change consistently in basal mammary epithelial cells upon vimentin knockdown

Previous studies in the laboratory suggested that pMLC2 could still be an informative marker in the assessment of primary human mammary epithelial cell (HMEC) contractility *in vitro* (Sonja Vahlman, 2021). HMECs demonstrate higher vimentin expression than mouse mammary epithelial cells (Figure 13).

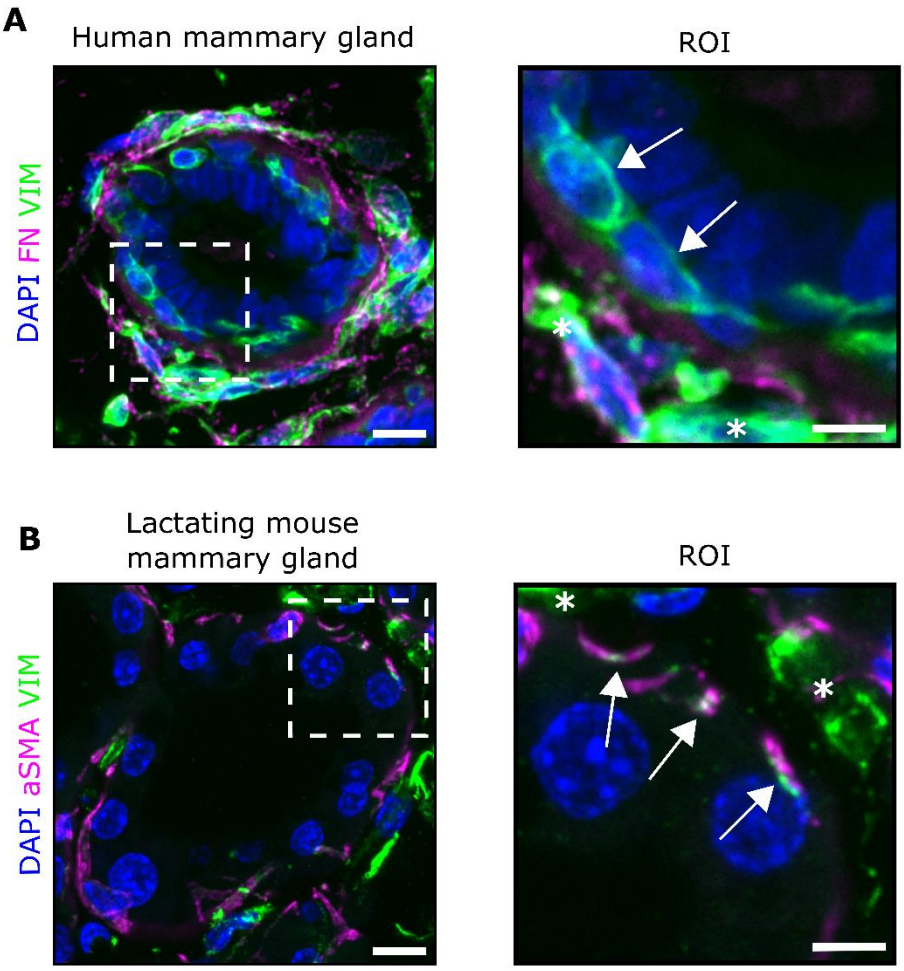


**Figure 13: Human basal epithelial cells exhibit higher vimentin expression than mouse basal epithelial cells.** Vimentin (VIM, green) positive (A) human basal mammary epithelial cell and (B) mouse basal mammary epithelial cells (arrows). (A) Human mammary gland acini stained for fibronectin (FN, magenta) (Image by Oona Paavolainen). (B) The basal epithelial cells of lactating mouse mammary gland alveoli were stained for alpha-smooth muscle actin (aSMA, magenta). In both images the cell nucleus was stained with DAPI (blue) and stars indicate stromal cells. Scale bar 10 µm, and 5 µm in region of interest (ROI).

A successful knockdown of vimentin with lentiviral short hairpin RNA (shRNA) compared to control shRNA was confirmed in two independent experiments done with two different breast reduction tissue samples (Figure 14) (Table 2). As cell contractility is strongly influenced by its mechanical and biochemical environment (Schedin & Keely, 2011), soft hydrogels corresponding to the approximate

stiffness of the mammary gland (1.6 kPa) were coated with relevant extracellular matrix (ECM) ligands, collagen I (col I), fibronectin (FN) or laminin-521 (Lm521) (Hu et al., 2017; Schedin & Keely, 2011). Shortly, these ECM ligands have different roles in mammary gland growth and differentiation and are abundant in different sites of the breast. For example, there is an abundance of col I in the breast stroma, where the fibrillar protein provides structural support and strength to the mammary gland (Brownfield et al., 2013; Schedin & Keely, 2011). Fibronectin in turn is located outside the basement membrane, and it has a role in the ECM stiffness (Hu et al., 2017; Schedin & Keely, 2011). The basement membrane is rich in laminin and thus mammary epithelial cells have a direct contact with Lm521 proteins (Avagliano et al., 2020; Englund et al., 2021; Schedin & Keely, 2011). Ongoing research conducted at our lab suggests, that different mammary gland epithelial cells prefer adhesion to different ECM ligands *in vitro*: luminal epithelial cells are most abundant when plated on Lm 521 and both luminal and basal cells adhere well on col I, but neither prefer FN (Englund et al., 2022).

Freshly isolated HMECs were lentivirally transduced and plated on the hydrogels for two days. HMEC basal cells [integrin alpha 6 positive ($ITGA6^+$) and/or keratin negative ($K8^-$)] and pMLC2 were labelled by immunofluorescence, and pMLC2 levels were quantified by image analysis (Figure 15).

Table 2: Clinical information of the breast reduction sample donors

| Experiment | Age at breast reduction | Kids | BMI | Oestrous cycle phase |
|---|---|---|---|---|
| 1. | 36 | 2 | 26.99 | Luteal phase |
| 2. | 43 | 2 | 25.78 | Hormonal contraception |

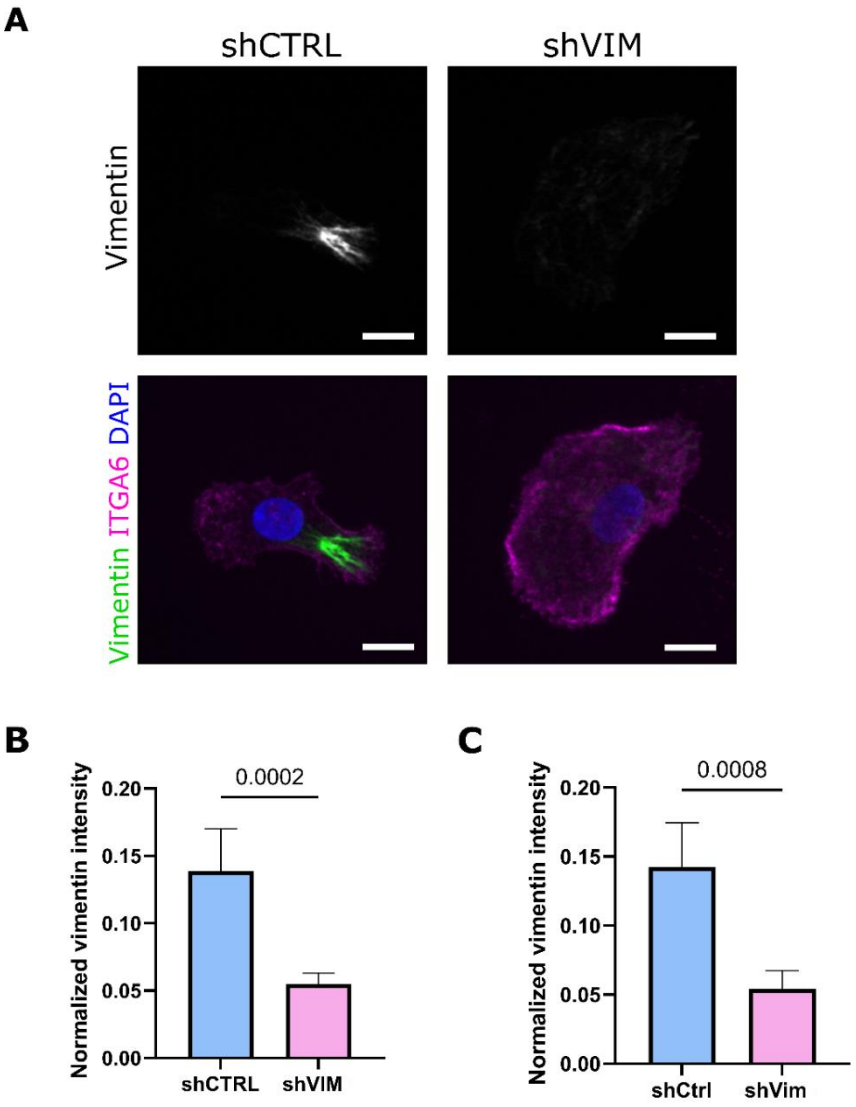


**Figure 14: Lentiviral knockdown**. (A) Vimentin (green) was knocked-down in human mammary epithelial cells using shCtrl and shVim lentiviruses. The vimentin signal was analysed, and the vimentin knockdown was perceived as being successful in both (B) experiment 1 ($n_{shCTRL}$= 36 and $n_{Vim}$= 50 cells) and (C) experiment 2 ($n_{shCTRL}$= 38 and $n_{Vim}$= 48 cells). Data presented as column graphs with mean ± SEM.

Even though vimentin knockdown was successful (Figure 14A-C), the effect of vimentin downregulation on MLC2 phosphorylation was inconsistent in the two independent experiments (Figure 15). In the first experiment, vimentin knockdown led to statistically significant decrease in pMLC2 in basal epithelial cells plated on col I and Lm521, but no difference was observed on FN (Figure 15B) (p=0.0072, two sample t-test; p=0.0009, Mann-Whitney test, respectively). In turn MLC2 phosphorylation was elevated in the second experiment on col I and FN (Figure 15C). However, the increase was statistically significant only in cells that were plated on fibronectin (p=0.0327, Mann-Whitney test). The overall pMLC2 levels were lower in the second experiment.

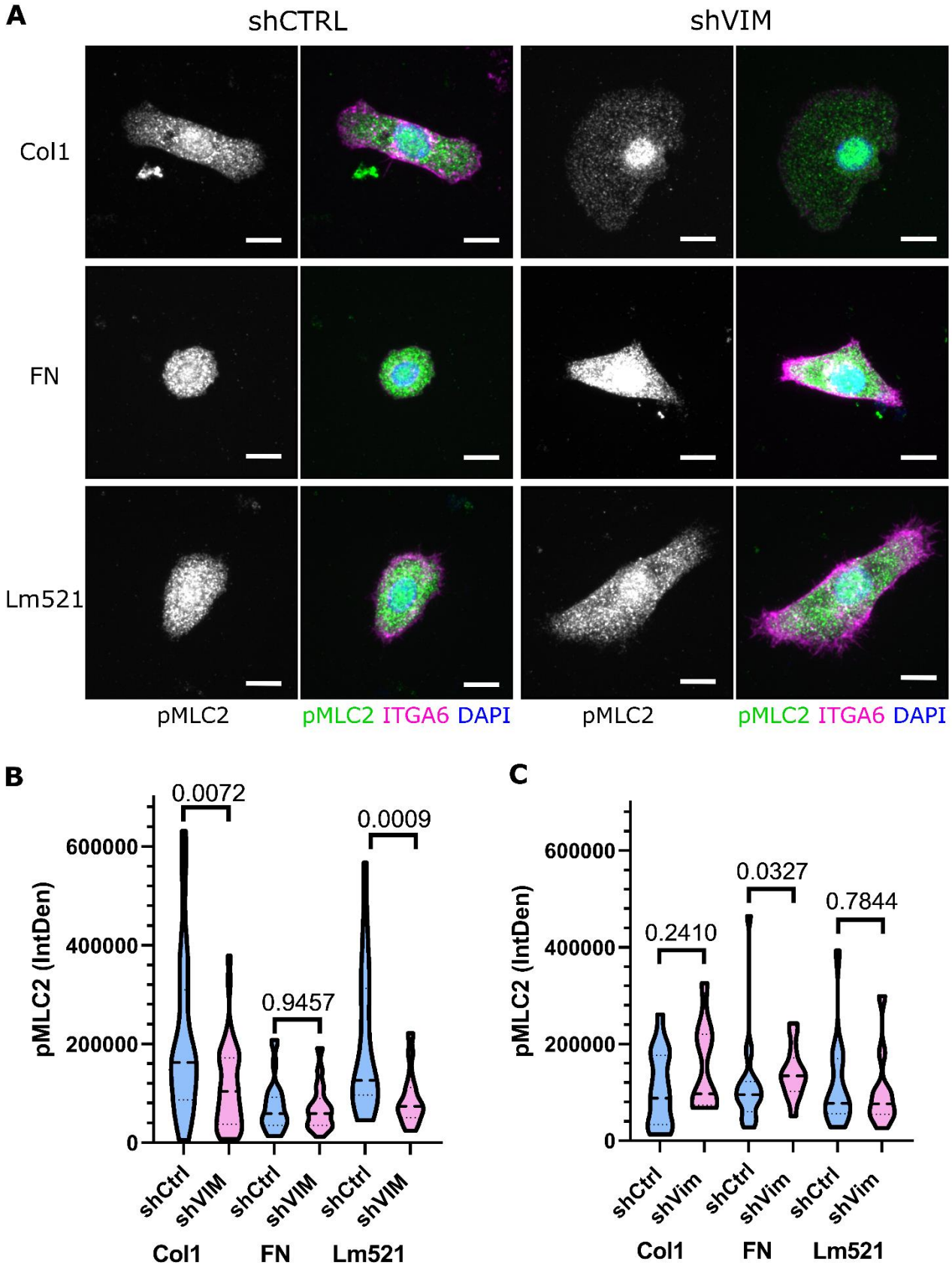


**Figure 15: Myosin-light chain phosphorylation does not change consistently in human basal mammary epithelial cells upon vimentin knockdown.** (A) Phosphorylation of myosin-light chain II (pMLC2) in primary human mammary basal epithelial cells [integrin alpha 6 positive (ITGA6$^{+}$)] after lentiviral vimentin knockdown was investigated in two individual experiments. Scale bar: 10 µm. (B) In the first experiment the pMLC2 signal

decreased upon vimentin knockdown ($n_{shCTRL}$= 19 – 32 cells and $n_{Vim}$= 26 – 41 cells) and (C) in the second experiment it increased ($n_{shCTRL}$= 13 – 20 cells and $n_{Vim}$= 9 – 13 cells). Data presented as violin plots where dashed line represent the mean and thinner dashed lines the lower and upper quartiles.

# 4 Discussion

## 4.1 Challenges in *Vim*$^{-/-}$ mice breeding might be caused be phenotypes other than defective lactation

The relationship between in mammalian litter size, lactation capacity, and body weight gain in the offspring is complex. The results of this study indicate that some *Vim*$^{-/-}$ female mice have reduced litter size compared with WT dams even though the result was not statistically significant. However, it is important to bear in mind that only the litters resulting from successful pregnancies are compared, and the unsuccessful breeding attempts were not taken into account in this study. Therefore, there may be a survival bias where the female mice that fail to breed are overlooked. Still, the observations made by several laboratories about the variation in *Vim*$^{-/-}$ dams' breeding capacity support the idea that vimentin deficiency might cause inability to produce live offspring in some *Vim*$^{-/-}$ dams. Nonetheless, it is still uncertain in why vimentin deficiency affects the breeding capacity of only some individuals.

As reduced mouse litter size could be related to difficulties in lactation, this hypothesis was investigated in *Vim*$^{-/-}$ mice. The lactation performance has been shown to be complex and multifactorial, which is why its relationship with litter size has remained unclear. It has been suggested that the mammary gland total mass, and thus milk yield, is adjusted to the litter size trough the number of placentas that induce lactogenic activity (Bateman, 2009; Nagasawa & Yanai, 1971). However, other studies suggest that lactation performance also depends on multiple factors occurring after gestation, such as temperature, energy intake and milking frequency (Duah et al., 2013). In other words, milk yield can be adjusted to demand. The pups also compete with each other for milk (Bateman, 2009; Stockley & Parker, 2002), and decreased feeding competition during nursing increases the weight gain in small litters (Knight et al., 1986; Parra-Vargas et al., 2020). Therefore, it is plausible that the reduced litter sizes of some *Vim-/-* dams could somehow compensate for an impaired lactation performance. For example, it could be speculated that the reduced litter sizes might lead to lesser demand for the differentiating and lactating mammary gland, and thereby the effect is not as evident as if it was in dams with larger litters. In all, it is challenging to evaluate, which aspects caused by vimentin deficiency could be linked to litter size or lactation performance in *Vim*$^{-/-}$ mice.

Importantly, no obvious defects in nursing were observed in this study upon vimentin deficiency. The visible milk spots in the stomach of the pups, and the preliminary data regarding the body weight of pups during the course of lactation suggest that the WT or heterozygous pups are feeding and gain

weight at similar rate. Therefore, vimentin deficiency in the dams does not cause obvious defects in nursing, or as stated above, the defects caused by the lack of vimentin might be compensated for by other mechanisms (such as reduced litter size). Prior studies have shown that vimentin facilitates lipolysis (Shen et al., 2010) and that vimentin deficiency leads to decreased weight gain and body fat accumulation in adult mice (Wilhelmsson et al., 2019). Therefore, vimentin deficiency might affect the energy available for breeding and nursing capacity, or even the composition of milk in *Vim*$^{-/-}$ dams. In addition, it is possible that the weight gain is impaired in the vimentin homozygous pups, independent of the nursing capacity of the dam.

It can also be speculated that the fluctuation in breeding capacity and litter sizes in *Vim*$^{-/-}$ female mice is not related to the lactation performance of the mammary gland but rather to other phenotypic characteristics or defects in other tissues. Interestingly, vimentin has been shown to regulate vascular endothelium, implying that vimentin deficiency could lead to decreased breeding capacity through impaired angiogenesis and vascular remodelling during placentation (Antfolk et al., 2017; Van engeland et al., 2019). In other words, vimentin deficiency might disturb placentation and lead to early termination of pregnancy in some dams.

Taken together, the breeding capacity of *Vim*$^{-/-}$ mice is likely susceptible to several factors and requires further research to truly evaluate the role of vimentin. To address the specific contribution of vimentin in the lactation, the litters of WT and *Vim*$^{-/-}$ dams should be cross-fostered and the litter size normalised for follow up of pup weight gain. Since vimentin deficiency has been shown to also affect fat accumulation, the phenotype of the dam and the pups need to be considered individually. Nonetheless, based on this study, challenges in lactation are likely not the primary reason for reduced *Vim-/-* breeding capacity.

## 4.2 Vimentin deficiency increases the alveolar size distribution in the lactating mammary gland

Upon pregnancy, the mammary gland undergoes carefully orchestrated and extensive proliferation and differentiation, which results in fully functional mammary gland (Hassiotou & Geddes, 2013; McNally & Stein, 2017). Overall vimentin expression was shown to increase during lactation in the human mammary gland as compared to non-lactating mammary gland (Michalczyk et al., 2001), assumably relating to the increased demand in cellular activity, such as milk ejection or metabolic transportation, in basal epithelial cells. The increased expression level might also suggest that

vimentin has a role in mammary gland development and differentiation, possibly relating to stress tolerance. Therefore, the effect of vimentin deficiency on lactogenic differentiation was investigated in this research project. In accordance with Peuhu et al. (2017) where vimentin deficiency did not prevent the alveologenesis of the mammary gland, no obvious defects were observed in the histology of the lactating *Vim*$^{-/-}$ mouse mammary gland. However, a larger variation in the alveolar size and tissue organization was noted compared to WT mammary gland during lactation. Although the H&E stained WT and *Vim*$^{-/-}$ lactating mammary gland sections seemed visually distinct, the average alveolar size was comparable, and we were not able to quantify the difference by image analysis. However, there are several possible sources of uncertainty in the tissue sampling and image analysis that might obscure the quantification results. Firstly, some of the tissue sections might have been cut at different location of the tissue piece or at a tilted orientation, because the sample fixation obscures the mammary gland leading it to compress and lose anatomical conformation. Secondly, image analysis based on morphological segmentation does not account for different tissue compartments. That is, also other structures than alveoli might have been measured.

Still, the results could also suggest that vimentin deficiency causes abbreviations in mammary gland morphogenesis. Previously, vimentin has been shown to be central in cell growth, motility and stress tolerance (Danielsson et al., 2018; Pattabiraman et al., 2020; Patteson, Pogoda, et al., 2019). For example, by providing mechanical tolerance and strength vimentin protects the nucleus during migration, and thus regulates cell motility and nuclear morphology in mouse embryonic fibroblasts (Patteson, Pogoda, et al., 2019; Patteson, Vahabikashi, et al., 2019). Moreover, in differentiating murine embryonic stem cells vimentin has been shown to have a pro-survival role that manifests during stress, and the vimentin deficiency leads to decreased neuronal differentiation (Pattabiraman et al., 2020). Therefore, vimentin might also have a protective role during mammary gland differentiation during pregnancy and lactation, and the lack of vimentin manifests as disrupted morphology.

Interestingly, Haaksma et al. (2011) found that also the alveoli of mice lacking alpha-smooth muscle actin (αSMA), a myoepithelial protein related to contractility, seemed consistently larger when compared to WT at the second day of lactation. Moreover, the lack of αSMA was discovered to impair lactating mammary gland contractile function without any major structural defects, and was hypothesised to be linked to the reduced milk ejection (Haaksma et al., 2011). In addition, only little milk could be seen in the stomachs of pups nursed by αSMA-deficient dams (Haaksma et al., 2011). Like vimentin, αSMA is part of the cell cytoskeleton and participates in cell contraction (Hinz et al., 2001). Therefore, similarly to αSMA, also vimentin might regulate mammary gland alveolar size

trough contractility. However, Haaksma et al. did not quantify the alveolar size, which is why their results cannot be directly compared to our results.

Similarly to αSMA-deficient lactating mammary glands, Peuhu et al. (2017) found that vimentin-deficient non-lactating mammary gland duct lumen appeared larger. They proposed that enlarged lumens might be a result of reduced proportion of basal epithelial cells, which could possibly also affect the lactating mammary gland alveoli lumen size. Thus, the proportion of epithelial cells in lactating *Vim*$^{-/-}$ mammary glands should be studied in order to conclude whether vimentin affects the lactating mammary gland morphology and ability to contract trough cell number. Moreover, reduced basal cell number could affect the mammary gland differentiation capacity in repeated pregnancies as *Vim*$^{-/-}$ mammary glands were also shown to have reduced regenerative capacity in a mammary gland transplant model (Peuhu et al., 2017).

Even though intermediate filaments are typically seen as the cell scaffolds that give the cells essential structural support, they are also important in cell signalling. For example, vimentin has been shown to act as an essential signal coordinator and regulator, for example in wound healing (Ostrowska-Podhorodecka & McCulloch, 2021; Ridge et al., 2022). Therefore, it is also plausible that irregular patterns and disorganization seen in the lactating *Vim*$^{-/-}$ mammary gland result from insufficient coordination during differentiation. Especially, since vimentin is absent in all tissues in *Vim*$^{-/-}$ mice, including the stromal cells, the interplay between mammary epithelial cells and stroma might be disturbed during differentiation. Surrounding stroma has previously been suggested to participate in epithelial cell organisation and modulation in the differentiating mammary gland (Schedin & Hovey, 2010). In addition, the ECM acts as a scaffold for epithelial cell growth and differentiation (Schedin & Hovey, 2010) and provides paracrine and mechanical signals (Avagliano et al., 2020; Hu et al., 2017). Hence, *Vim*$^{-/-}$ mice might have disturbances in cell signalling that affect the mammary gland morphology. Moreover, vimentin-deficient adipocytes have been reported to be smaller in size (Shen et al., 2010), which might affect their role in providing metabolites or local differentiation cues for the growing epithelium (Hovey & Aimo, 2010). However, the relationship between vimentin and adipocytes, and the relationship's possible impact on mammary gland differentiation remains an interesting topic to be studied.

Altogether, vimentin has been shown to have several roles in different cell types of epithelial and mesenchymal origin, which provides a challenge in distinguishing the impact of vimentin deficiency in differentiating mammary gland. Thus, cell type or tissue specific knockout of vimentin would allow to pinpoint more precisely the role of vimentin in mammary epithelial cells. Nonetheless, the results

of this study show that the mammary gland function is secured, and vimentin deficiency does not drastically interfere with lactation. In other words, the adaptive capacity of the mammary gland possibly compensates for the loss of vimentin.

## 4.3 Vimentin regulates the accumulation of milk lipid droplets in luminal mammary epithelium

The lipid droplets in milk are a notable source of nutrition and bioactive components for the mammalian neonates. The milk lipid droplet production, composition, movement and secretion are highly complex processes that depend on, for example, milk ejection, lactation stage and diet of the dam (Mather et al., 2019). As we hypothesized that vimentin regulates lactation, the effect of vimentin deficiency on epithelial milk lipid droplets was investigated in histological samples. Interestingly, larger but fewer lipid droplets were observed in lactating *Vim*$^{-/-}$ mice mammary gland epithelial cells when compared to WT. This could indicate that the vimentin deficiency causes problems in releasing milk through contraction. Decreased frequency of milk-let downs has been speculated to lead to lipid droplet accumulation at the apical surface of the milk-producing epithelial cells and, thus, an increase in the size of the lipid droplets (Mather et al., 2019; Stemberger et al., 1984). In other words, vimentin-deficient mammary glands might contract less or with lower frequency, giving more time for the lipid droplets to accumulate and fuse within the milk-secreting epithelial cells. However, even though the *Vim*$^{-/-}$ pups' milk spots ensured that they had been recently fed, the exact time-point of nursing was not controlled, which might have affected the results. In addition, the altered morphology of the vimentin-deficient mammary gland might also make it more challenging to contract properly, and thereby affect the milk lipid accumulation within the luminal epithelium. Taken together, vimentin might affect the mammary gland contractile function, reflected on the milk lipid droplet size and number.

There are, however, several other possible explanations to these results. The lipid droplet size is strongly related to their composition. For example, milk lipid droplets rich in phosphatidylethanolamines promote droplet fusion while membrane phosphatidylcholines stabilise the milk lipid droplet surface and supress fusion (Cohen et al., 2015; Mather et al., 2019; Walter et al., 2020). In addition, large lipid droplets can grow by adding locally synthesised triacylglycerols to the lipid core (Wilfling et al., 2013). It has been previously reported that vimentin plays a role in the lipid droplet formation and lipolysis in adipocytes (Franke et al., 1987; Shen et al., 2010; Wilhelmsson et al., 2019). Therefore, it is plausible that vimentin deficiency could affect lipid droplet size through

altered lipid homeostasis. However, luminal epithelial cells do not express detectable levels of vimentin, which is why direct association between vimentin and milk lipid droplet formation in luminal epithelial cells is unlikely. Instead, vimentin might affect milk lipid droplet composition by regulating fat metabolism elsewhere. For example, vimentin affects cholesterol mobilization for steroidogenesis (Shen et al., 2012), and vimentin IFs interact with hormone-sensitive lipase, an enzyme that breaks down triglycerides stored in adipose tissue and thus mobilizing the free fatty acids (Shen et al., 2010). Altered steroidogenesis and lipolysis in vimentin-deficient mice might lead to abnormal plasma levels of different milk lipid droplet components, which in turn might affect the milk lipid droplet growth in mammary epithelium. In cultured bovine mammary epithelial cells the milk lipid droplet size was not affected by the cellular triglyceride amount, but rather the type of triglyceride precursor available (Cohen et al., 2015). The triglyceride precursors also affected the phospholipid content of the lipid membrane and thus their susceptibility for droplet fusion. No significant differences were observed in the lipid droplet size and number within the alveolar lumen of WT and *Vim*$^{-/-}$ mammary glands, suggesting that the fusion rate of the secreted milk lipid droplets is comparable. In other words, the composition of fusion regulating membrane phospholipids, namely phosphatidylethanolamine and phosphatidylcholine, is likely not altered in vimentin-deficient mammary epithelium. Nonetheless, whilst milk lipid droplet composition has been extensively studied, many questions regarding the relationship between the composition and movement of milk lipids remain unanswered. Taken together, the relationship between vimentin and milk lipid droplet composition is complex and warrants further investigation.

Another scenario that could affect the lipid droplet size in vimentin-deficient mice is altered ovarian and adrenal steroidogenesis. Vimentin is involved in the cholesterol movement from lipid droplets to mitochondria, where progesterone steroidogenesis takes place, and vimentin ablation has been shown to decrease the progesterone serum levels while still retaining the oestrus cycle (Shen et al., 2012). Progesterone is essential in alveologenesis and side branching of mammary glands (Lydon et al., 1995), but it's role in milk production is obscure. In cows, progesterone has been found to regulate milk lipid droplet size, but not milk yield, in a very low density lipoprotein (VLDL) –dependent manner (Argov-Argaman et al., 2020). Consistently with this study, there was no difference in the total area of milk lipid droplets between WT and *Vim*$^{-/-}$ mouse mammary gland sections, which further supports the idea that progesterone is not involved in the regulation of the milk yield. In cows, the milk lipid droplets were larger when progesterone levels were decreasing during the oestrus cycle, but no specific correlation between progesterone concentration and lipid droplet size was found (Argov-Argaman et al., 2020). Therefore, lower total progesterone levels in vimentin-deficient mice

(Shen et al., 2012) might not be linked to the increased milk lipid droplet size observed in this study. However, as these hypotheses have not been investigated specifically during pregnancy or early lactation, we cannot rule out that vimentin regulates milk lipid droplets size and number in a progesterone-dependent manner. Altogether, vimentin might affect lactation trough progesterone production, but further work is required to truly establish their relationship.

A limitation of these results is that the lipid droplets with a diameter less than approximately 0.5 μm could not be measured, because of the inadequate image resolution. Most of the lipid droplets are smaller than 1 μm in diameter, while the lipid droplets with the diameter of 1 – 8 μm account for the majority of the lipid volume (Masedunskas et al., 2017; Mather et al., 2019). Thus, the unintentional absence of tiny milk lipid droplets in the analysis might have some effect on the droplet count, but probably had only little effect on the average size. Furthermore, the specificity and sensitivity of Nile red stain to different lipids were not considered, which might have caused some bias in the results. Nile red stains particularly neutral lipids, such as triglycerides and cholesteryl esters, but can also bind more weakly, for example, phospholipids (Greenspan et al., 1985). Moreover, other lipids in the staining environment affect the fluorescence intensity of Nile red: the presence of VLDL favours greater fluorescence intensity over high density lipoprotein (Greenspan et al., 1985). Therefore, if the milk lipid droplet fat content is altered between the phenotypes, the Nile red signal intensity might be slightly different in stained WT and *Vim*$^{-/-}$ mammary gland sections.

Taken together, the effect of vimentin on milk lipid droplet size and count might be related to altered basal epithelial cell function and/or milk content (Figure 16). However, dynamic studies with the focus on mammary gland contraction frequency in response to oxytocin are needed to establish the role of vimentin in basal epithelial cell function during lactation.

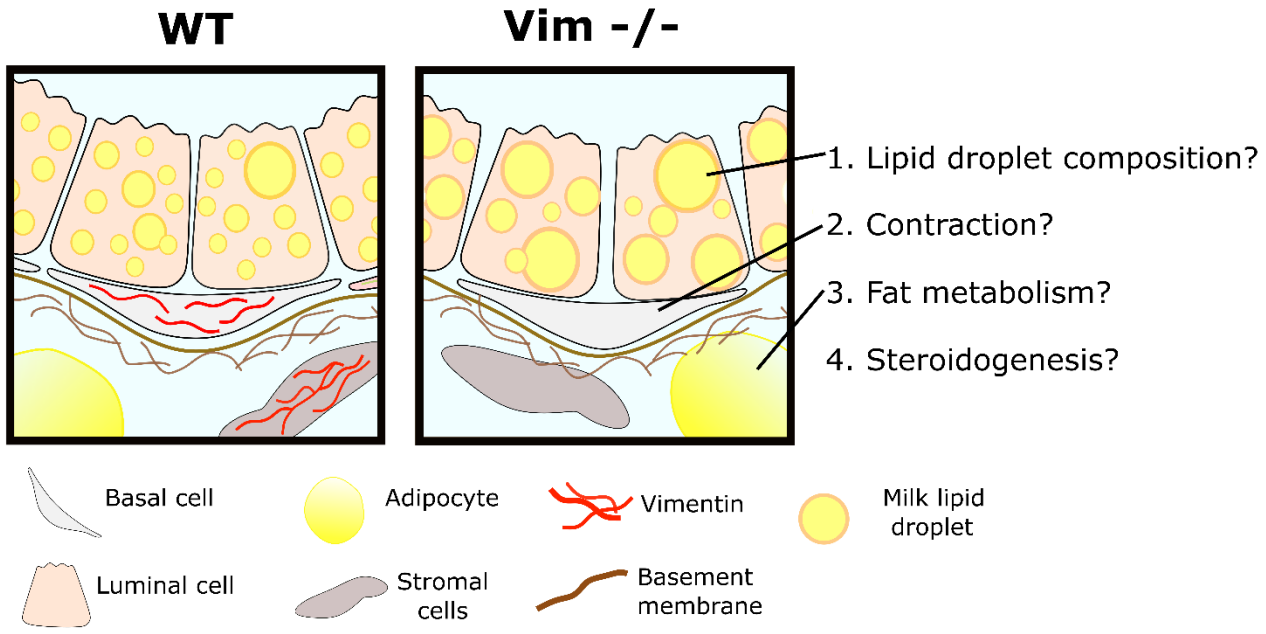


**Figure 16: Overview of how vimentin might affect milk lipid droplet size and number.** Vimentin deficiency might affect milk lipid droplet size and number trough (1) altered lipid droplet composition and homeostasis, (2) reduced contraction frequency or magnitude, (3) altered fat metabolism in adipose tissue or (4) reduced steroidogenesis.

## 4.4 Myosin-light chain 2 phosphorylation has limited applicability in the analysis of mammary gland contraction

In response to neonate suckling, the posterior pituitary releases oxytocin, which initiates contraction of mammary gland basal epithelial cells upon binding to the oxytocin receptor on these cells (Gieniec & Davis, 2022; Gimpl & Fahrenholz, 2001). This oxytocin stimulated contraction of mammary basal epithelial cells is essential for milk ejection from the alveolar lumen trough the mammary ductal system all the way to the nipple (Adriance et al., 2005; Tortora & Bryan, 2014). Several cytoskeletal components are involved in generating the forces required for the cell contraction (Adriance et al., 2005; Gieniec & Davis, 2022). As vimentin levels increase during lactation (Michalczyk et al., 2001) and vimentin has been shown to regulate cell contraction and to provide the cell flexibility and resistance to tensile forces (Eckes et al., 1998; Jiu et al., 2017), we hypothesized that vimentin might also be involved in basal epithelial cell contractility.

In this research project, the role of vimentin in basal mammary epithelial cell contraction was investigated by analysing the phosphorylation of myosin-light chain II, which has been reported to correlate with cell contractility (Olins & Bremel, 1982; Vasquez & Martin, 2016). However, the changes in MLC2 phosphorylation were inconsistent upon vimentin knockout or lentiviral silencing.

Although non-lactating mouse mammary gland exhibited clear pMLC2 signal in the basal cells, no specific pMLC2 signal could be detected in the tissue sections of a lactating mouse mammary gland. This is contrary to the findings of Raymond et al. (2011) and Stevenson et al. (2020), who showed pMLC2 signal in lactating mammary glands. However, Raymond et al. could only detect a weak signal in the immunohistochemically stained mammary gland sections, and they also confirmed the pMLC2 expression by immunoblotting. Moreover, Stevenson et al. (2020) stimulated their samples with oxytocin right prior to fixation, and the signal was still not uniform across the basal epithelial cells due to asynchronous contraction. This could indicate that only a small level of MLC2 is phosphorylated in the relaxed lactating mouse mammary gland, which is why it might be challenging to detect, especially without more sensitive methods. Taken together, only a very low level of MLC2 phosphorylation could be detected in the lactating mouse mammary gland in the absence of oxytocin stimulation and, therefore, the role of vimentin in the regulation of pMLC2 levels in the mammary gland could not be explored further. Nonetheless, Stevenson et al. (2020) showed that the lactating mammary gland contracted in response to oxytocin even when MLCK and few other components of the contractile pathways were pharmacologically inhibited. Thus, they suggest that there are other possible pathways that could compensate for MLC phosphorylation controlled contraction (Stevenson et al., 2020), which could also explain why we only saw a very low level of pMLC2 in lactating mammary glands.

Furthermore, in vimentin-silenced primary HMECs, the MLC2 phosphorylation levels were contradictory in the two independent experiments. This inconsistency in the results could be explained by different factors affecting the data. Firstly, the mammary gland tissue is inevitably heterogenous across breast reduction donors, which causes variability in the results. While the two sample donors were similar in terms of age, weight and parity, other factors such as different menstrual cycle phase could affect the cells and their behaviour *in vitro* (Table 2). The fluctuation in oestrogen and progesterone has been shown to regulate, for example, cell differentiation and mammary gland epithelium proliferation (Murrow et al., 2022; Nazário et al., 1994). However, the effect of menstrual cycle on mammary gland epithelial cells' contractile function has not been investigated and remains as an interesting issue for the future studies. Secondly, the breast ECM is highly dynamic and heterogeneous among individuals (Murrow et al., 2022) and regulates mammary epithelial cells by guiding their growth and differentiation (Hu et al., 2017; Murrow et al., 2022). Thus, the individual ECM characteristics of the original breast tissue could affect the initial HMEC adhesion *in vitro*, and also reflect the mechanosensing capacity of the cells on different ECM ligands. In other words, the cells might be adjusted to different microenvironments and therefore behave

contradictory *in vitro*. More experimental replicates with the same patient sample could, for example, aid in clarifying the results.

Importantly, the breast reduction donors were not breastfeeding at the time of surgery nor were the cells induced towards lactating phenotype *in vitro*. Therefore, the pMLC2 signal in the vimentin knockdown experiments might better reflect the cells' contraction potential and their ability to contract during diverse, non-lactation related cellular functions, such as cell differentiation or tissue remodelling (Vicente-Manzanares et al., 2009). Taken together, the results of HMEC experiments cannot be directly translated to the lactating stage.

There are some sources of uncertainty related to the methods used in this study, which might also explain the obscurity of the results. For example, the used cell markers and cell typing were not optimal. Firstly, the cell markers used in the two independent experiments were different. The first experiment depended on distinguishing the basal epithelial cells from luminal epithelial cells based mainly on the luminal marker, keratin 8, while in the second experiment also a basal epithelial marker, integrin alpha 6, was used for distinguishing the cell types from each other. Secondly, some bleed trough of the fluorescence signal from an adjacent channel was detected in confocal microscopy in the first experiment (image not shown). Thus, the cell typing was considerably more challenging in the first experiment, and was improved in the second experiment.

Furthermore, MLC2 phosphorylation was not the ideal readout for investigating the mammary basal epithelial cells' ability to contract. Although the phosphorylation of MLC2 is known to initiate cell contraction (Vasquez & Martin, 2016) and has been previously utilised as a readout for lactating mouse mammary gland contractile function, no pMLC2 signal could be detected in the basal epithelial cells of the lactating mouse mammary gland it this research project. Moreover, the pMLC2 analysis results of HMECs was inconsistent. In the study by Raymond et al. (2011), also the non-phosphorylated myosin light-chain was labelled, which exhibited a clear signal. This approach could have been utilised for evaluating the proportion of myosin light-chains that had been phosphorylated. Finally, labelling of pMLC2 describes the engagement of the signalling pathway underlying the cell contraction, and does not inform about the dynamic ability of the cells to contract (Mroue et al., 2015). Thus, the role of vimentin in providing the cells with mechanical strength and flexibility is overlooked in this type of experimental setup.

In fact, measuring dynamic events like contractility in fixed cell or tissue samples is challenging, and live cell or *ex vivo* imaging is required for understanding these phenomena. In the future studies, the role of vimentin in cell contraction should be investigated in real time, for example, by investigating

vimentin-deficient mammary gland contraction in response to oxytocin in isolated mammary glands *ex vivo*, or *in vivo* using intravital imaging in live mice. Especially, the novel intravital imaging technique of surgically exposed mouse mammary gland developed by Masedunskas et al. (2017), is a promising approach for investigating the mammary gland movement, and could be utilised for investigating basal epithelial cell contractility at an advanced level. Moreover, also real time imaging of oxytocin induced mammary gland organoid models might offer fundamental insight in the epithelial cell contractile function. Alternatively, the mouse mammary gland could be induced with oxytocin just before isolating and fixating the mammary glands and the mammary alveoli diameter could be compared between the phenotypes as described in the paper by Haaksma et al. (2011). Though in this method, the effect of the phenotype on the tissue morphology must be carefully considered to not misinterpret the results. All in all, there are several alternative research methods and an increasing number of new technologies for studying the contractile function of cells.

Taken together, these results did not reveal possible changes in the contraction of mammary epithelial cells upon vimentin silencing or knockout. Therefore, further research is required to investigate the role of vimentin in mammary basal epithelial cell contraction during lactation. Preferably, future studies should utilise real time methods and investigate the contractile function in response to oxytocin stimulation.

# 5 Conclusion

In this master's thesis the role of vimentin in mammary gland morphology and basal epithelial cell contractility was investigated. The *Vim*$^{-/-}$ mammary gland showed disorganised morphology and variation in alveolar size, but the lactating mammary gland function was not drastically affected, which indicates that the mammary gland has adaptive capacity that compensates for any defects related to the loss of vimentin and secures lactation. However, the high variation responses between healthy human HMEC samples obscures the analysis, which is why direct conclusions could not be made regarding basal epithelial cell contractility. Nevertheless, milk lipid droplets were accumulated in the *Vim*$^{-/-}$ mammary gland as compared to WT mammary gland, which suggest that vimentin is involved in milk lipid droplet release from the milk producing luminal cells. Alternatively, vimentin might also have a role in fat metabolism in the context of milk production.

The role of vimentin in lactation might become obvious first when the mammary gland is challenged, and therefore future studies need to address the ability of *Vim*$^{-/-}$ mammary gland to undergo repeated pregnancies. Moreover, tissue or cell type –specific ablation of vimentin would allow to rule out systemic effects on mammary gland differentiation and function caused by a full vimentin knockout. Importantly, vimentin in mammary gland contractility should be explored in real time so that the dynamic of vimentin in force generation could be better evaluated.

Taken together, vimentin is involved in mammary gland differentiation and function, but the exact role remains unclear. Still, as vimentin is often upregulated in cancer, and many differentiation processes are also altered during breast cancer progression, it is essential to understand the normal mammary gland function to understand pathophysiology behind breast cancer. Altogether, research of vimentin in mammary epithelial cell contractility can be informative for understanding the normal function of mammary gland as well as breast cancer and its progression, and thereby be useful in guiding the development of suitable therapeutics.

# 6 Methods

## 6.1 Mice

Vimentin knock-out and wild type female mice in a mixed FVB/N, sv129 and C57Bl/6 background were used and housed under standard laboratory conditions receiving food and water ad-libitum. For the experiments, mice were sacrificed with carbon dioxide and cervical dislocation, and left and right thoracic and abdominal mammary glands were harvested (Figure 17). Age matched nine-week-old mice were used for investigating non-lactating mouse mammary glands. The mammary glands from dams' first pregnancy on their first lactation day (L1) (i.e., the morning after birth) were harvested for investigating lactating mouse mammary glands. Also, pups were investigated for white milk spots i.e., their stomach is full of milk. In all experiments mice compared were up to three generations apart. All animal studies were ethically conducted (Animal license number ESAVI/36583/2020) and carried out in the accordance with the Finnish Act on Animal Experimentation while following the principle of three Rs.

The abdominal mammary glands were dissected and stretched on an objective glass to adhere followed by fixation in Carnoy's medium (60% ethanol, 30% chloroform, 10% glacial acetic acid) overnight (o/n) at +4 °C, after which they were stored in 70% ethanol. The left thoracic mammary glands were dissected and fixed in PLP-buffer (Periodate-Lysine-Paraformaldehyde, pH 7.4; For recipe see appendix 2) o/n at +4 °C, washed twice with P-buffer (for recipe see appendix 3) and stored until mounting in 30% sucrose (Merck, 107687) in P-buffer. For frozen tissue sections, samples were mounted in Tissue-Tek® O.C.T. Compound (Sakura, 4583) on dry ice and tissue blocks stored in –80 °C. The frozen tissue sections and haematoxylin and eosin (H&E) staining was provided by Histocore at the University of Turku.

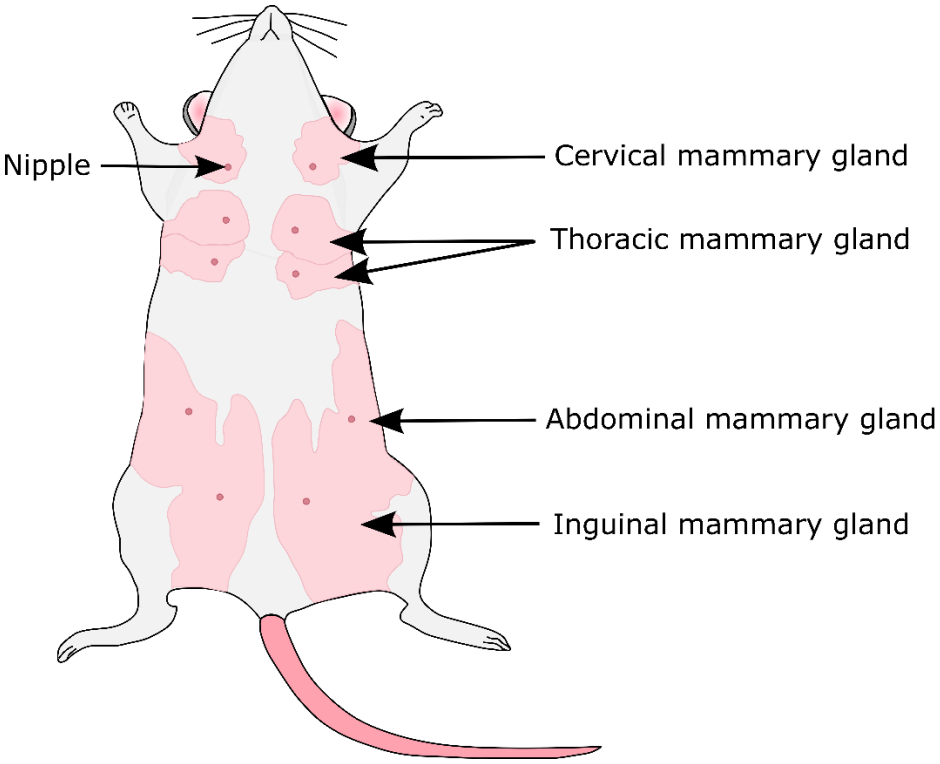


**Figure 17**: Anatomy of mouse mammary glands. Mice have five pairs of mammary glands.

## 6.2 Whole mount staining

The abdominal mouse mammary gland fixed in Carnoy's medium and stored in 70% ethanol were rehydrated at room temperature (RT) in decreasing ethanol concentrations of 50% and 25% for 20 minutes each and lastly in water for 10 minutes. The samples were stained with Carmine alum [0.2% carmine (Sigma-Aldrich, C0122), 0.5% aluminium potassium sulphate dodecahydrate Sigma-Aldrich] o/n at RT, and then washed and dehydrated in increasing ethanol concentrations of 70 %, 95 % and 100 % for 30 minutes each at RT. The samples were cleared in xylene (AnalaR NORMAPUR® ACS, VWR Chemicals, 28975.360) for three days and mounted in Permount mounting medium (Mount Agent Pertex®, Histolab Products, 00811) and let dry o/n at RT prior to imaging.

## 6.3 Immunofluorescence staining of tissue sections

H&E staining was provided by Histocore and performed using Leica Autostainer automated slide stainer. The H&E stained slides were scanned using Pannoramic P1000 Slide Scanner (3DHISTECH Ltd. Budapest, Hungary).

Prior to staining the frozen mouse mammary gland sections were permeabilised and blocked with 0.1% Triton™ X-100 (Sigma-Aldrich, T8787) in 2 % bovine serum albumin (BSA; Biowest, P6154) dissolved in phosphate-buffered saline (PBS) for 30 minutes.

For immunohistochemical (IHC) staining the tissue sections were incubated with primary antibodies (Table 3) in 2% BSA for 1 hour RT, washed with PBS and incubated with fluorochrome-conjugated secondary antibodies diluted to 1:400 (Table 4) for 1 hour RT. For milk lipid droplet staining the L1 mouse mammary gland sections were stained with Nile red (concentration 1 mM, used dilution 10 µM; Sigma-Aldrich, 19123) and phalloidin-Atto 647N (used dilution 1:600; Sigma-Aldrich, 65906) for 1 hour RT. Nile red stains intracellular lipids (Greenspan et al., 1985) and phalloidin binds the cytoskeletal actin filaments (filamentous actin; F-actin) (Lengsfeld et al., 1974; Wulf et al., 1979). Sections were washed with PBS, nuclei stained with 4′,6-diamidino-2-phenylindole (DAPI) (dilution 1:1000) in PBS, washed with water, and mounted in Mowiol containing DABCO (Calbiochem, Merck Millipore, 47590) and let dry in dark o/n at RT.

**Table 3**: Primary antibodies used for mouse mammary gland section immunohistochemical staining

| Experiment | Antibody | Host species | Catalogue number and manufacturer | Used dilution |
|---|---|---|---|---|
| Mouse IHC | Monoclonal Anti-Actin, α-Smooth Muscle | Mouse | A2547-.2ML Sigma-Aldrich | 1:500 |
| | Keratin, type II/ Cytokeratin 8 | Rat | TROMA-I-c Hybridoma Bank | 1:1000 |
| | Vimentin (D21H3) XP® | Rabbit | 5741S Cell Signaling Technology | 1:100 |
| | Anti-Myosin light chain (phospho S20) antibody | Rabbit | ab2480 Abcam | 1:200 |
| | Phospho-Myosin Light Chain 2 (Thr18/Ser19) Antibody | Rabbit | 3674S Cell Signaling Technology | 1:100 |

**Table 4**: Secondary antibodies. The dilution 1:400 was used for all secondary antibodies.

| Secondary antibody (Used dilution 1:400) | Conjugate | Host species | Catalogue number and manufacturer |
|---|---|---|---|
| Anti-mouse IgG | Alexa Fluor 488 | Donkey | A21202 Invitrogen |
| Anti-rabbit IgG | Alexa Fluor 488 | Donkey | A21208 Invitrogen |
| Anti-rat IgG | Alexa Fluor 568 | Goat | A11077 Invitrogen |
| Anti-mouse IgG | Alexa Fluor 647 | Donkey | A31571 Invitrogen |
| Anti-rabbit IgG | Alexa Fluor 647 | Donkey | A31573 Invitrogen |

## 6.4 Polyacrylamide hydrogel preparation

Polyacrylamide (PAA) hydrogels of 1.6 kPa stiffness were prepared on glass-bottom petri dishes (Mattek, P35G-1.0-14-C, 35mm dish, 14 mm Microwell). The dishes were treated with 3-(trimethoxysilyl)propyl methacrylate binding solution (Fisher, 10422411) in acetic acid and 96% ethanol for 30 minutes at RT. The binding solution was removed, and the dishes were washed twice with 96% ethanol. The prepared hydrogels contained 40 % acrylamide solution (BioRad Laboratories, A4058) and 2% Bis acrylamide solution (Biorad Laboratories, M1533) in PBS. Ammonium persulfate (APS) (10% w/v solution, BioRad Laboratories) and N,N,N′,N′-tetramethyl ethylenediamine (Sigma-Aldrich, T-9281) were added to the solution to start the polymerization. The final solution was pipetted on top of the glass-bottom dishes and the droplet was covered with 13 mm coverslip. The gels were incubated 1 h at RT, whereafter PBS was added to the glass-bottom petri-dishes and the coverslips were carefully removed. The smoothness of the gels was confirmed with a light microscope and the gels were stored in + 4 °C immersed in PBS for up to 2 weeks.

For the purpose of surfaces of hydrogels were activated with 1 mg/ml Sulfo-SANPAH (Sigma-Aldrich, 803332) and 10 mg/ml EDC (N-(3-Dimethylaminopropyl)-N′-ethylcarbodiimide hydrochloride, Sigma-Aldrich, 03450) in 50 mM HEPES (pH 7.5, Sigma-Aldrich, H0887-100ML) for 30 minutes at RT on slow agitation. Then, the gels were incubated in UV-oven for 10 minutes to photo-activate the cross-linker Sulfo-SANPAH and washed with PBS three times for 10 minutes.

Hydrogels were coated o/n at + 4 °C with either collagen 1 (5 mg/ml, Merck Millipore, 08-115), laminin-521 (1 mg/ml, Thermo Scientific, A29248) or fibronectin (0.1 mg/ml, Merck Millipore, 341631) in 1ml PBS with the final concentration of 5 µg/ml.

## 6.5 Primary human mammary epithelial cell isolation

Primary human mammary epithelial cells (HMECs) are regularly isolated at Peuhu lab as a standard procedure and stored in – 150 °C. Human breast tissue is obtained upon informed consent from reduction mammoplasty surgeries conducted at Turku University Hospital (Ethical approval ETMK 23 /1801/2018).

Previously isolated HMECs were thawed by suspending cells in warm mammary epithelial cell growth medium (MEGM; Promocell, C-21010) and centrifuging at 600 g for 3 min at +4 °C. Epithelial cell containing pellet was resuspended in warm trypsin-ethylenediaminetetraacetic acid (EDTA) (0.25%, Gibco, 25200–056) and the mixture was moved to a BSA-coated well to avoid cell attachment. Cell-trypsin mixture was incubated at +37 °C for 15-20 minutes while observing the cell cluster dissociation every 5 min until obtaining a single-cell suspension. Trypsinisation was inactivated by adding warm MEGM on the cells and centrifuging at 600 g for 3 min at +4 °C. The pellet was resuspended in a 1:1 Dispase (5 mg/ml, Roche, 4942078001) – 10µg/ml DNAase 1 (Roche, 11284932001) in MEGM mixture, pipetted continuously for one minute and centrifuged at 600 g for 3 min at +4 °C. Lastly, the pellet was resuspended in MEGM and filtered through a 40 µm cell strainer (Falcon, 352340) and cells counted with a Bürker counting chamber (NanoEnTek).

## 6.6 Lentiviral gene silencing

The expression of vimentin was knocked down using lentiviral transfection with vectors containing short hairpin RNA (shRNA). Vimentin shRNA sequences were as follows:

VIM TRCN0000029123 (shVIM):

CCGGGACAGGTTATCAACGAAACTTCTCGAGAAGTTTCGTTGATAACCTGTCTTTTT

Moreover, a shRNA control vector (shCTRL) was used (Sigma-Aldrich, MISSION pLKO.1-puro Non-Mammalian shRNA Control Plasmid DNA, SHC002).

One million HMECs were suspended in virus mixtures [shCTRL and shVIM 1 x 108 TU/ml (MOI=1)] and incubated in suspension on low adhesion 24 wells plates for 16 hours. Then, the cell mixture was collected into falcons and each well washed with an additional 1 ml of warm MEGM which was also collected to the falcons. The collected mixture was centrifuged at 600 g for 3 minutes, the pellet was resuspended in 1 ml trypsin-EDTA, incubated in RT for 10 min and mixed gently to separate cell clusters into single cells. The mixture was centrifuged, and the pellet was resuspended

in 1 ml MEGM for cell counting. 20 000 cells in 200 µl MEGM were plated on each PAA hydrogel and incubated for 1 hour at 37 °C for cells to adhere. Finally, PAA hydrogels were topped up with 1.3 ml MEGM. Cells were cultured for two days, after which they were fixed with 4 % PFA for 10 min in RT, washed with PBS and stored in 4°C until further use.

## 6.7 Human mammary epithelial cell immunofluorescence

All HMECs on PAA hydrogels were stained for basal and luminal epithelial cell markers. Knockdown (KD) control samples plated on collagen 1 coated PAA hydrogels were also stained for vimentin.

Prior to staining the cells were permeabilised with 0.1 % Triton-X in PBS for 10 min at RT and blocked with blocking buffer (10% horse serum in 0.1 % Tris Buffered Saline with Tween (TBST) for 1 hour at RT. Cells were incubated in primary antibodies (Table 5) in blocking buffer overnight at +4 °C and washed with PBS. Then, cells were incubated with fluorochrome-conjugated secondary antibodies (Table 4) in blocking buffer for 1 hour at RT on a shaker and washed with PBS. Cell nuclei were stained with DAPI (dilution 1:1000) for 5 mins at RT and washed with PBS on a shaker. The cells were immersed in PBS and stored at + 4 °C until imaging.

**Table 5:** Primary antibodies used in human mammary epithelial cell immunofluorescence

| | Antibody | Host species | Catalogue number and manufacturer | Used dilution |
|---|---|---|---|---|
| HMEC IHC | Keratin, type II/ Cytokeratin 8 | Rat | TROMA-I-c Hybridoma Bank | 1:1000 |
| | Keratin 14 Polyclonal Antibody | Rabbit | 905301 Biolegend | 1:1000 |
| | Vimentin (D21H3) XP® | Rabbit | 5741S Cell Signaling Technology | 1:100 |
| | Anti-Myosin light chain (phospho S20) antibody | Rabbit | ab2480 Abcam | 1:200 |
| | Human Integrin alpha 6/CD49f Alexa Fluor® 405-conjugated Antibody | Mouse | FAB1350V-100UG R&D systems | 0.2 mg/ml |

## 6.8 Microscopy

The H&E stained slides were scanned using Pannoramic P1000 Slide Scanner (3DHISTECH Ltd. Budapest, Hungary).

The Carmine alum-stained mouse mammary gland whole mounts were imaged with Zeiss Axio Zoom.V16 stereomicroscope (Carl Zeiss AG, Oberkochen, Germany) equipped with Zeiss Axiocam 105 colour -camera and 1.0x/0.125 NA PlanApo Z objective using CL 9000 LED CAN ring light and visiLED MC1000 as light sources and controlled with the Zen Pro-software. The images were captured using exposure time of 10 ms. The whole gland was imaged using 7x magnification in 2-3 frames, and a mosaic image was generated automatically with PhotoShop (versio, Adobe Inc. Adobe Photoshop, California, USA) of each gland using these images. 20x and 40x magnifications were used for taking close-up images.

Stained mouse mammary gland frozen sections and HMECs were imaged using 3i Marianas CSU-W1 spinning disk (50µm pinholes) confocal microscope (Intelligent Imaging Innovations Inc., Denver, Colorado, USA) equipped with a Zeiss Axio Observer 7 Advanced Marianas Z1 (Carl Zeiss AG, Oberkochen, Germany) -inverse microscope, Prime BSI Scientific sCMOS (Photometrics, Tucson, Arizona, USA) -camera and 3i LaserStack- lasers, and using the Slidebook 6 software (3i Intelligent Imaging Innovations Inc., Denver, CO). Images were captured with Zeiss Plan-Apochromat 63x/1.40 NA oil objective and Zeiss Plan-Apochromat 20x/0.8 NA air objective. Lasers of 405 nm, 488 nm, 561 nm and 640 nm wavelengths were used for excitation and the emission light was collected with 445/45 nm, 525/30 nm, 617/73 nm and 692/40 nm filters, respectively. For all imaging Z-stacks were captured: frozen tissue sections were imaged using stack size of 5-10 planes with z-step thickness of 2 µm, and HMECs using stack size of 20-30 planes with z-step thickness of 0.5 µm.

## 6.9 Image analysis

ImageJ– software (version 1.53q) (Schindelin et al., 2012) was used for image analysis.

The alveolar size of H&E stained L1 mouse mammary glands was quantified using FIJI MorpoLipJ plugin (Legland et al., 2016). First, MRXS images were exported to TIFF with zoom level 1:16 in CaseViewer version 2.4 (3DHISTECH Ltd., Budapest, Hungary). In ImageJ a representative area of 3000 µm x 3000 µm was selected from each L1 mammary gland section (Figure 18A). A

morphological segmentation was done to the representative areas and the particles of the size of 100 – 40 000 µm were analysed after watershed segmentation (Figure 18B, C).

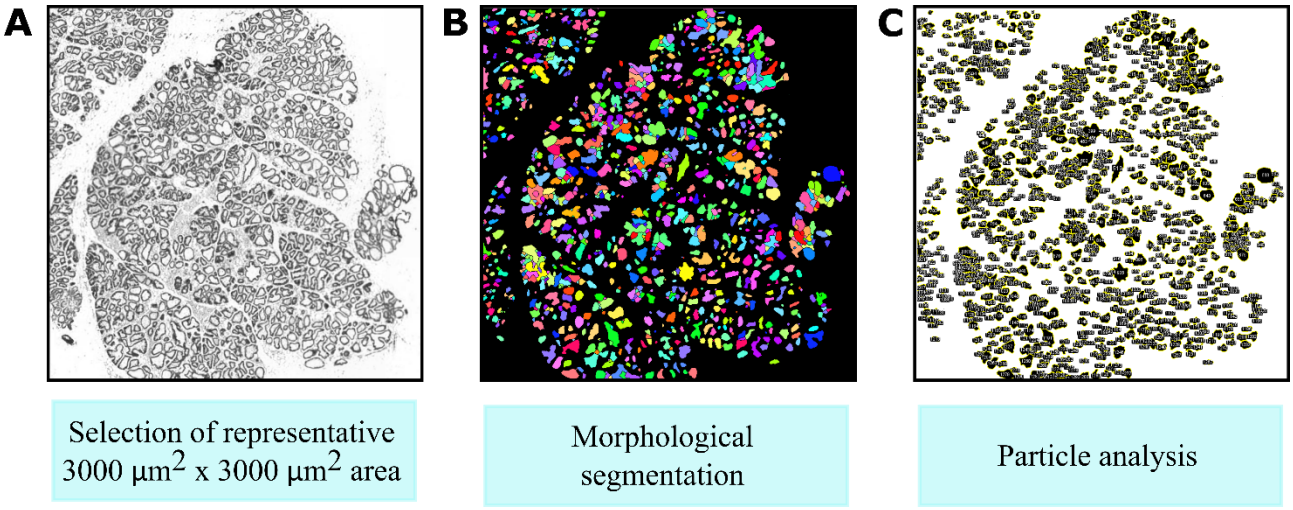


**Figure 18: Analysis of L1 mammary gland alveolar size.** (A) A representative area of the day 1 mouse mammary glands was selected and (B) a morphological segmentation was done in ImageJ using MorphoLipJ plugin. (C) Lastly watershed segmentation of the image was conducted and the particles of the size of 100 – 40 000 µm were analysed.

The size and number of lipid droplets within the L1 mouse mammary gland epithelium and alveolar lumen was quantified. First, a maximum intensity projection of three middle slices of both 20x magnification phalloidin and Nile red channels was obtained. Utilising phalloidin signal (Figure 19A), masks were created to first segment total glandular area from stroma (Figure 19B), and then to distinguish epithelial area within the gland (Figure 19C). Thereafter, the lipid droplet count and number were analysed from the Nile red signal (Figure 19D) by thresholding the image based on the visible lipids signal and by using particle analysis (Figure 19E, F). Additionally, the mammary gland, mammary epithelium and mammary alveolar lumen areas were measured. The lipid droplet area and count were normalised using the total epithelial or alveoli lumen area prior to statistical analysis.

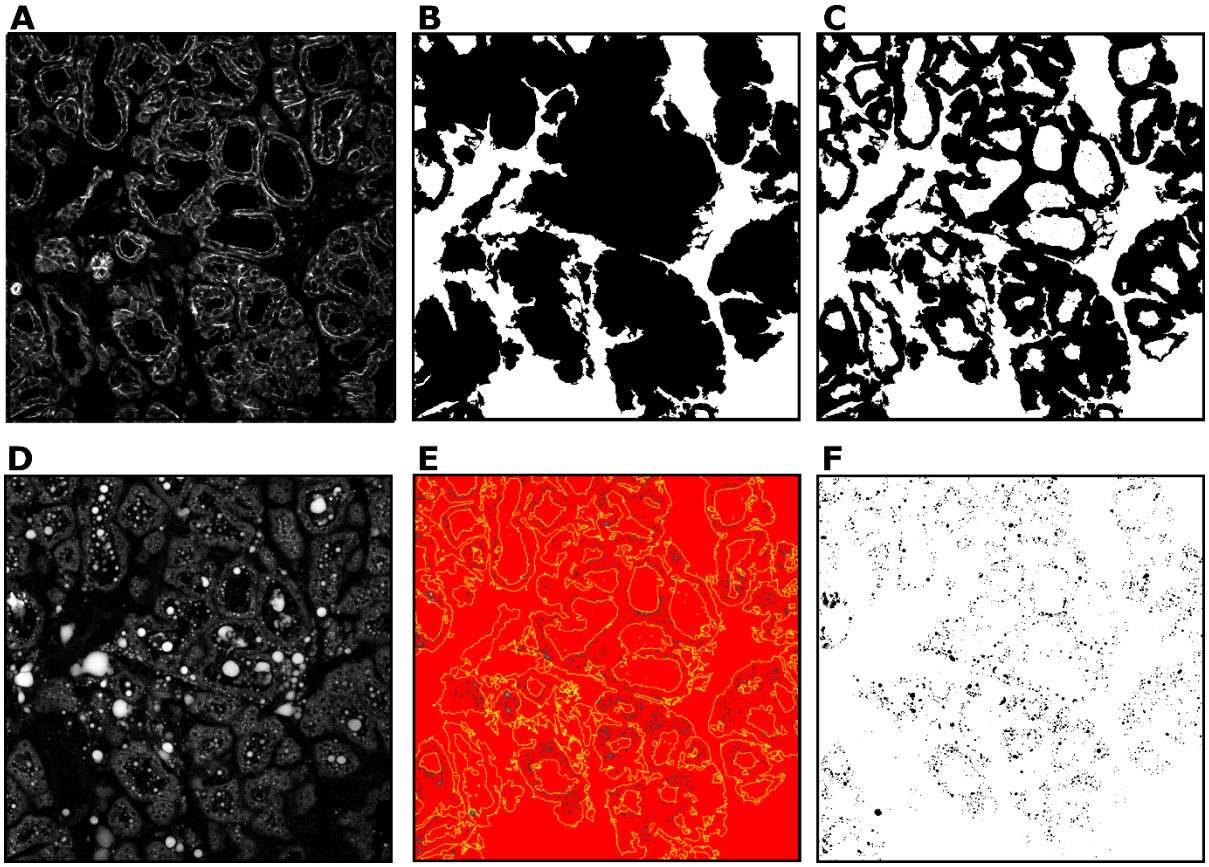


**Figure 19: Lipid droplet analysis workflow in ImageJ.** For quantifying milk lipid droplet size and number (A) phalloidin signal was used for creating mask of (B) total glandular area and (C) epithelial area of the gland. The lipid droplet average size and number were analysed from (D) the Nile red signal by (E and F) thresholding the lipid droplets within the mammary gland epithelial area. The lipid droplet size and number within the alveolar lumen was similarly quantified.

To study vimentin's effect on pMLC2 levels, the pMLC2 signal intensity was quantified. A selection of 20-25 HMEC cells were selected in an unbiased manner by only viewing their nuclei, and imaged. Cell types as well as vimentin and pMLC2 signal intensity was analysed for each cell from maximum intensity projection. For cell typing the brightness and contrast was set to the same and the cell types were categorized based on their expression of different cell markers by visual scoring (Table 6 and Table 7). The vimentin and pMLC2 signal intensity was measured from each cell separately. Using a macro, the cell area was chosen and only the signal intensity within the cell area was measured (Figure 20).

**Table 6:** Cell typing in the first experiment.

| **Experiment 1** | **Keratin 8** | **Keratin 14 (only KD proof)** |
|---|---|---|
| **Luminal** | Positive | Negative |
| **Basal** | Negative | Positive |
| **Stromal** | Negative | Negative |

**Table 7:** Cell typing in the second experiment.

| Experiment 2 | Keratin 8 | Human integrin alpha 6 |
|---|---|---|
| **Luminal** | Positive | Low or negative |
| **Basal** | Negative | High or positive |
| **Stromal** | Negative | Low or negative |

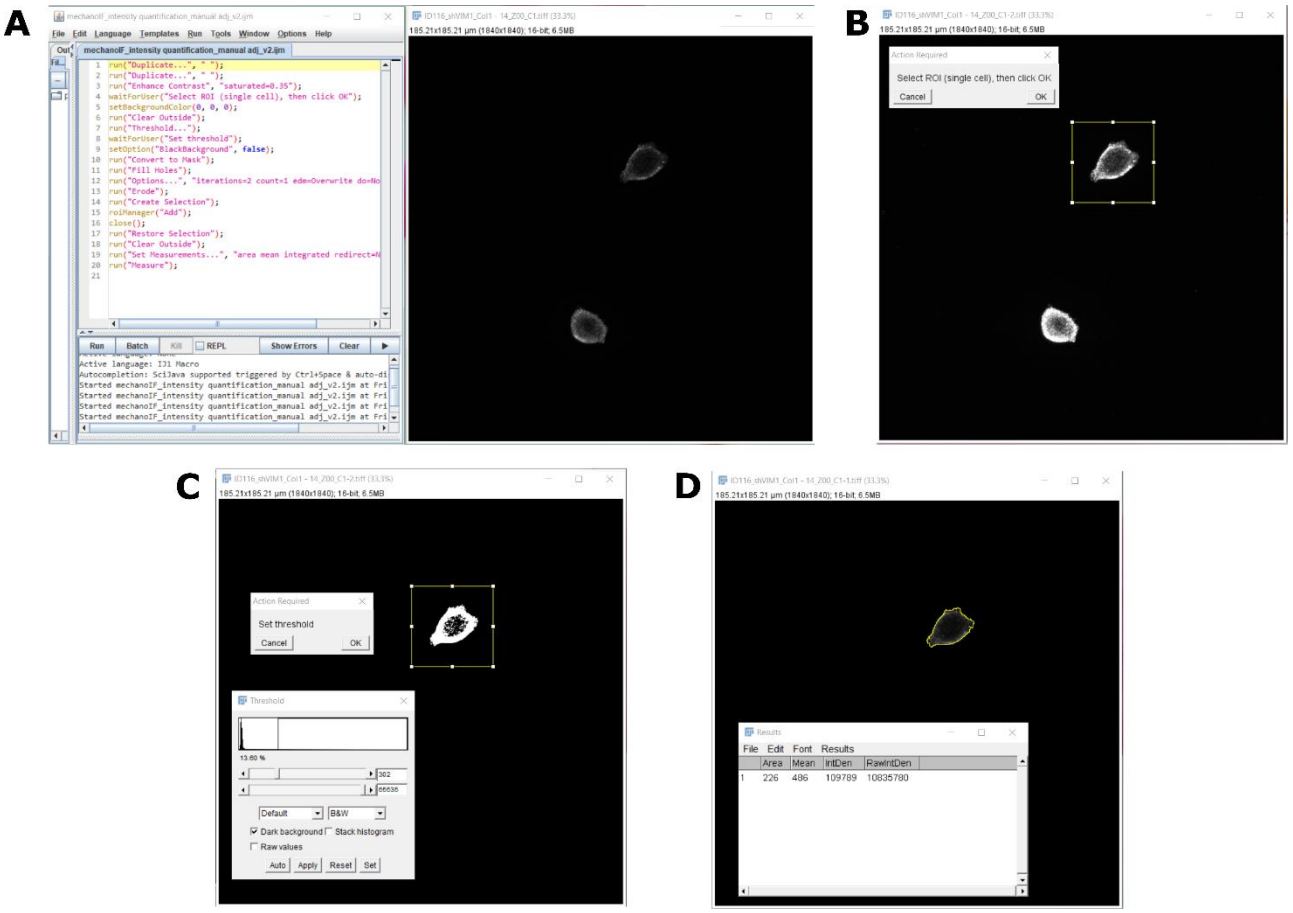


**Figure 20: Vimentin and phosphorylated myosin-light chain signal analysis workflow in ImageJ.** (A) View of the used macro and maximum intensity projection image. (B) A single cell was selected and (C) a threshold for that cell was set for selecting the cell area. (D) The signal intensity within the cell area was then measured.

## 6.10 Statistical analysis

GraphPad Prism version 8.4.2 (GraphPad Software, San Diego, California USA, www.graphpad.com) was used for statistical analyses. The data was tested for normality using Shapiro-Wilks normality test and also evaluated visually. Normally distributed data was analysed

using two-sided unpaired t-test, and non-parametric two-sided Mann-Whitney U-test was used when data did not pass the test for normality.

For assessment of vimentin knockdown efficiency, vimentin signal was normalised by dividing each vimentin signal value with the highest value of the control group. Moreover, the number of milk lipid droplets and total area of milk lipid droplets were normalised by the mammary gland epithelium area.

Data presented in column graphs are shown with means and standard error of the mean (SEM) and data presented in violin blots are shown with means and with lower and upper quartile. Column graphs and violin plots are presented also with p-values, and statistically significant p-values were considered less than 0.05.

## Acknowledgements

I wish to sincerely thank my supervisor Emilia Peuhu for her guidance and expertise throughout the master's thesis research project. I thank you for giving me an opportunity to explore the mammary gland and showing how fascinating organ it truly is. I greatly thank my second supervisor Oona Paavolainen for teaching me various methods and for patiently answering my endless questions in the lab. You gave me valuable lessons in imaging, and by throwing me in at the deep end of microscoping you gave me important confidence in my own skills. I also wish to thank Peuhu lab members Defne Dinc, Markus Peurla and Leena Koskinen for offering invaluable advice and a helping hand with the experiments.

Moreover, I wish to express my gratitude to the women that consented to the use of their breast tissue for research purposes after they underwent reduction mammoplasty surgeries, and the Turku University Hospital personnel that conducted the surgeries.

Lastly, I would like to thank my wonderful friends and family for believing in me and for supporting me through the whole master's thesis process. Thank you for always being there and for listening to my endless ramble. The years as a university students would not have been the same without your presence and encouragement.

## List of abbreviations

| | |
|---|---|
| αSMA | Alpha-smooth muscle actin |
| ATPase | Adenosine 5'-triphosphatase |
| BSA | Bovine serum albumin |
| Col I | Collagen I |
| DAPI | 4′,6-diamidino-2-phenylindole |
| DNA | Deoxyribonucleic |
| ECM | Extracellular matrix |
| EDTA | Ethylenediaminetetraacetic acid |
| ETM | Epithelial–mesenchymal transition |
| F-actin | Filamentous actin |
| FN | Fibronectin |
| H&E | Haematoxylin and eosin |
| HMEC | Human mammary epithelial cell |
| IF | Intermediate filaments |
| IHC | Immunohistochemistry |
| ITGA6 | Integrin alpha 6 |
| K8 | Cytokeratin 8 |
| KD | Knockdown |
| KO | Knock-out |
| L1 | Lactation day 1 |
| Lm521 | Laminin-521 |
| MEGM | Mammary epithelial cell growth medium |
| MLC | Myosin light-chain |
| MLC2 | Myosin light-chain II |
| MLCK | Myosin light-chain kinase |
| o/n | Overnight |

| | |
|---|---|
| PAA | Polyacrylamide |
| pMLC2 | Phosphorylated myosin-light chain II |
| RNA | Ribonucleic acid |
| ROCK | Rho-associated protein kinase |
| ROI | Region of interest |
| RT | Room temperature |
| shCtrl | shRNA control vector |
| shRNA | Short hairpin RNA |
| shVIM | shRNA vimentin vector |
| SMA | Smooth muscle actin |
| TDLU | Terminal ductal-lobular unit |
| TEB | Terminal end bud |
| ULF | Unit-length filament |
| VIM | Vimentin |
| *Vim*$^{-/-}$ | Vimentin knockout |
| VLDL | Very low density lipoprotein |
| WT | Wild type |

## References

Adriance, M. C., Inman, J. L., Petersen, O. W., & Bissell, M. J. (2005). Myoepithelial cells: good fences make good neighbors. *Breast Cancer Research*, *7*(5), 190. https://doi.org/10.1186/BCR1286

Alberts, B., Johnson, A., Lewis, J., Martin, R., Roberts, K., & Walter, P. (2015). Chapter 16: The Cytoskeleton. In *Molecular Biology of The Cell* (6th ed.). Garland Science.

Antfolk, D., Sjöqvist, M., Cheng, F., Isoniemi, K., Duran, C. L., Rivero-Muller, A., Antila, C., Niemi, R., Landor, S., Bouten, C. V. C., Bayless, K. J., Eriksson, J. E., & Sahlgren, C. M. (2017). Selective regulation of Notch ligands during angiogenesis is mediated by vimentin. *Proceedings of the National Academy of Sciences of the United States of America*, *114*(23), E4574–E4581. https://doi.org/10.1073/PNAS.1703057114

Arendt, L. M., & Kuperwasser, C. (2015). Form and function: how estrogen and progesterone regulate the mammary epithelial hierarchy. *Journal of Mammary Gland Biology and Neoplasia*, *20*. https://doi.org/10.1007/S10911-015-9337-0

Argov-Argaman, N., Raz, C., & Roth, Z. (2020). Progesterone Regulation of Milk Fat Globule Size Is VLDL Dependent. *Frontiers in Endocrinology*, *11*. https://doi.org/10.3389/FENDO.2020.00596

Atwood, C. S., Hovey, R. C., Glover, J. P., Chepko, G., Ginsburg, E., Robison, J., & Vonderhaar, B. K. (2000). Progesterone induces side-branching of the ductal epithelium in the mammary glands of peripubertal mice. *The Journal of Endocrinology*, *167*(1), 39–52. https://doi.org/10.1677/JOE.0.1670039

Avagliano, A., Fiume, G., Ruocco, M. R., Martucci, N., Vecchio, E., Insabato, L., Russo, D., Accurso, A., Masone, S., Montagnani, S., & Arcucci, A. (2020). Influence of Fibroblasts on Mammary Gland Development, Breast Cancer Microenvironment Remodeling, and Cancer Cell Dissemination. *Cancers*, *12*(6), 1–35. https://doi.org/10.3390/CANCERS12061697

Bach, K., Pensa, S., Grzelak, M., Hadfield, J., Adams, D. J., Marioni, J. C., & Khaled, W. T. (2017). Differentiation dynamics of mammary epithelial cells revealed by single-cell RNA sequencing. *Nature Communications*, *8*(1). https://doi.org/10.1038/S41467-017-02001-5

Bateman, N. (2009). Some physiological aspects of lactation in mice. *The Journal of Agricultural Science*, *49*(1), 60–77. https://doi.org/10.1017/S0021859600034328

Battaglia, R. A., Delic, S., Herrmann, H., & Snider, N. T. (2018). Vimentin on the move: new developments in cell migration. *F1000Research*, *7*. https://doi.org/10.12688/F1000RESEARCH.15967.1

Brisken, C., Park, S., Vass, T., Lydon, J. P., O'Malley, B. W., & Weinberg, R. A. (1998). A paracrine role for the epithelial progesterone receptor in mammary gland development. *Proceedings of the National Academy of Sciences of the United States of America*, *95*(9), 5076. https://doi.org/10.1073/PNAS.95.9.5076

Brownfield, D. G., Venugopalan, G., Lo, A., Mori, H., Tanner, K., Fletcher, D. A., & Bissell, M. J. (2013). Patterned Collagen Fibers Orient Branching Mammary Epithelium through Distinct Signaling Modules. *Current Biology*, *23*(8), 703–709. https://doi.org/https://doi.org/10.1016/j.cub.2013.03.032

Centonze, A., Lin, S., Tika, E., Sifrim, A., Fioramonti, M., Malfait, M., Song, Y., Wuidart, A., Van Herck, J., Dannau, A., Bouvencourt, G., Dubois, C., Dedoncker, N., Sahay, A., de Maertelaer, V., Siebel, C. W., Van Keymeulen, A., Voet, T., & Blanpain, C. (2020). Heterotypic cell–cell communication regulates glandular stem cell multipotency. *Nature 2020 584:7822*, *584*(7822), 608–613. https://doi.org/10.1038/s41586-020-2632-y

Cohen, B. C., Shamay, A., & Argov-Argaman, N. (2015). Regulation of Lipid Droplet Size in Mammary Epithelial Cells by Remodeling of Membrane Lipid Composition—A Potential Mechanism. *PLoS ONE*, *10*(3). https://doi.org/10.1371/JOURNAL.PONE.0121645

Cole, H. A. (1933). The Mammary Gland of the Mouse, during the Oestrous Cycle, Pregnancy and Lactation. *Proceedings of the Royal Society of London. Series B, Containing Papers of a Biological Character*, *114*(787), 136–161. http://www.jstor.org/stable/81731

Colucci-Guyon, E., Portier, M. M., Dunia, I., Paulin, D., Pournin, S., & Babinet, C. (1994). Mice lacking vimentin develop and reproduce without an obvious phenotype. *Cell*, *79*(4), 679–694. https://doi.org/10.1016/0092-8674(94)90553-3

Cooper, A. P. (1840). *On the Anatomy of the Breast* (Vol. 1). Longman.

Cristea, S., & Polyak, K. (2018). Dissecting the mammary gland one cell at a time. *Nature Communications 2018 9:1*, *9*(1), 1–3. https://doi.org/10.1038/s41467-018-04905-2

Danielsson, F., Peterson, M. K., Araújo, H. C., Lautenschläger, F., Karin, A., Gad, B., Caldeira Araújo, H., Lautenschläger, F., & Gad, A. (2018). Vimentin Diversity in Health and Disease. *Cells*, *7*(10), 147. https://doi.org/10.3390/cells7100147

Dontu, G., & Ince, T. A. (2015). Of Mice and Women: A Comparative Tissue Biology Perspective of Breast Stem Cells and Differentiation. *Journal of Mammary Gland Biology and Neoplasia 2015 20:1*, *20*(1), 51–62. https://doi.org/10.1007/S10911-015-9341-4

Duah, O. A., Monney, K. A., Hambly, C., Król, E., & Speakman, J. R. (2013). Limits to sustained energy intake. XVII. Lactation performance in MF1 mice is not programmed by fetal number during pregnancy. *Journal of Experimental Biology*, *216*(12), 2339–2348.

https://doi.org/10.1242/JEB.078428

Eckes, B., Dogic, D., Colucci-Guyon, E., Wang, N., Maniotis, A., Ingber, D., Merckling, A., Langa, F., Aumailley, M., Delouvée, A., Koteliansky, V., Babinet, C., & Krieg, T. (1998). Impaired mechanical stability, migration and contractile capacity in vimentin-deficient fibroblasts. *Journal of Cell Science*, *111 ( Pt 13)*(13), 1897–1907. https://doi.org/10.1242/JCS.111.13.1897

Englund, J. I., Bui, H., Dinç, D. D., Paavolainen, O., McKenna, T., Laitinen, S., Munne, P., Klefström, J., Peuhu, E., & Katajisto, P. (2022). Laminin matrix adhesion regulates basal mammary epithelial cell identity. *Journal of Cell Science*, *135*(23). https://doi.org/10.1242/JCS.260232

Englund, J. I., Ritchie, A., Blaas, L., Cojoc, H., Pentinmikko, N., Döhla, J., Iqbal, S., Patarroyo, M., & Katajisto, P. (2021). Laminin alpha 5 regulates mammary gland remodeling through luminal cell differentiation and Wnt4-mediated epithelial crosstalk. *Development*, *148*(12). https://doi.org/10.1242/DEV.199281

Fletcher, D. A., & Mullins, R. D. (2010). Cell mechanics and the cytoskeleton. *Nature*, *463*(7280), 485. https://doi.org/10.1038/NATURE08908

Franke, W. W., Hergt, M., & Grund, C. (1987). Rearrangement of the vimentin cytoskeleton during adipose conversion: formation of an intermediate filament cage around lipid globules. *Cell*, *49*(1), 131–141. https://doi.org/10.1016/0092-8674(87)90763-X

Freeman, M. E., Kanyicska, B., Lerant, A., & Nagy, G. (2000). Prolactin: structure, function, and regulation of secretion. *Physiological Reviews*, *80*(4), 1523–1631. https://doi.org/10.1152/PHYSREV.2000.80.4.1523

Gan, Z., Ding, L., Burckhardt, C. J., Lowery, J., Zaritsky, A., Sitterley, K., Mota, A., Costigliola, N., Starker, C. G., Voytas, D. F., Tytell, J., Goldman, R. D., & Danuser, G. (2016). Vimentin Intermediate Filaments Template Microtubule Networks to Enhance Persistence in Cell Polarity and Directed Migration. *Cell Systems*, *3*(3), 252-263.e8. https://doi.org/10.1016/J.CELS.2016.08.007

Geddes, D. T. (2007). Inside the Lactating Breast: The Latest Anatomy Research. *Journal of Midwifery & Women's Health (JMWH)*, *52*(6), 556–563. www.jmwh.org

German, J. B., Dillard, C. J., & Ward, R. E. (2002). Bioactive components in milk. *Current Opinion in Clinical Nutrition and Metabolic Care*, *5*(6), 653–658. https://doi.org/10.1097/00075197-200211000-00007

Gieniec, K. A., & Davis, F. M. (2022). Mammary basal cells: Stars of the show. *Biochimica et Biophysica Acta. Molecular Cell Research*, *1869*(1). https://doi.org/10.1016/J.BBAMCR.2021.119159

Gimpl, G., & Fahrenholz, F. (2001). The oxytocin receptor system: Structure, function, and regulation. *Physiological Reviews*, *81*(2), 629–683. https://doi.org/10.1152/physrev.2001.81.2.629

Gouon-Evans, V., Rothenberg, M. E., & Pollard, J. W. (2000). Postnatal mammary gland development requires macrophages and eosinophils. *Development (Cambridge, England)*, *127*(11), 2269–2282. https://doi.org/10.1242/DEV.127.11.2269

Greenspan, P., Mayer, E. P., & Fowler, S. D. (1985). Nile red: a selective fluorescent stain for intracellular lipid droplets. *The Journal of Cell Biology*, *100*(3), 965. https://doi.org/10.1083/JCB.100.3.965

Haaksma, C. J., Schwartz, R. J., & Tomasek, J. J. (2011). Myoepithelial cell contraction and milk ejection are impaired in mammary glands of mice lacking smooth muscle alpha-actin. *Biology of Reproduction*, *85*(1), 13–21. https://doi.org/10.1095/BIOLREPROD.110.090639

Hassiotou, F., & Geddes, D. (2013). Anatomy of the human mammary gland: Current status of knowledge. *Clinical Anatomy*, *26*(1), 29–48. https://doi.org/10.1002/CA.22165

Hinz, B., Celetta, G., Tomasek, J. J., Gabbiani, G., & Chaponnier, C. (2001). Alpha-smooth muscle actin expression upregulates fibroblast contractile activity. *Molecular Biology of the Cell*, *12*(9), 2730–2741. https://doi.org/10.1091/MBC.12.9.2730/ASSET/IMAGES/LARGE/MK0911600008.JPEG

Hovey, R. C., & Aimo, L. (2010). Diverse and active roles for adipocytes during mammary gland growth and function. *Journal of Mammary Gland Biology and Neoplasia*, *15*(3), 279–290. https://doi.org/10.1007/s10911-010-9187-8

Hu, G., Li, L., & Xu, W. (2017). Extracellular matrix in mammary gland development and breast cancer progression. *Frontiers in Laboratory Medicine*, *1*(1), 36–39. https://doi.org/10.1016/J.FLM.2017.02.008

Huveneers, S., & Danen, E. H. J. (2009). Adhesion signaling - crosstalk between integrins, Src and Rho. *Journal of Cell Science*, *122*(Pt 8), 1059–1069. https://doi.org/10.1242/JCS.039446

Inman, J. L., Robertson, C., Mott, J. D., & Bissell, M. J. (2015). Mammary gland development: cell fate specification, stem cells and the microenvironment. *Development*, *142*(6), 1028–1042. https://doi.org/10.1242/DEV.087643

Jiu, Y., Lehtimäki, J., Tojkander, S., Cheng, F., Jäälinoja, H., Liu, X., Varjosalo, M., Eriksson, J. E., & Lappalainen, P. (2015). Bidirectional Interplay between Vimentin Intermediate Filaments and Contractile Actin Stress Fibers. *Cell Reports*, *11*(10), 1511–1518. https://doi.org/10.1016/J.CELREP.2015.05.008

Jiu, Y., Peränen, J., Schaible, N., Cheng, F., Eriksson, J. E., Krishnan, R., & Lappalainen, P. (2017).

Vimentin intermediate filaments control actin stress fiber assembly through GEF-H1 and RhoA. *Journal of Cell Science*, *130*(5), 892–902. https://doi.org/10.1242/jcs.196881

Knight, C. H., Maltz, E., & Docherty, A. H. (1986). Milk yield and composition in mice: effects of litter size and lactation number. *Comparative Biochemistry and Physiology. A, Comparative Physiology*, *84*(1), 127–133. https://doi.org/10.1016/0300-9629(86)90054-X

Kraxner, J., Lorenz, C., Menzel, J., Parfentev, I., Silbern, I., Denz, M., Urlaub, H., Schwappach, B., & Köster, S. (2021). Post-translational modifications soften vimentin intermediate filaments. *Nanoscale*, *13*(1), 380–387. https://doi.org/10.1039/D0NR07322A

Legland, D., Arganda-Carreras, I., & Andrey, P. (2016). MorphoLibJ: integrated library and plugins for mathematical morphology with ImageJ. *Bioinformatics*, *32*(22), 3532–3534. https://doi.org/10.1093/BIOINFORMATICS/BTW413

Lengsfeld, A. M., Löw, I., Wieland, T., Dancker, P., & Hasselbach, W. (1974). Interaction of phalloidin with actin. *Proceedings of the National Academy of Sciences of the United States of America*, *71*(7), 2803–2807. https://doi.org/10.1073/PNAS.71.7.2803

Liu, C.-Y., Lin, H.-H., Tang, M.-J., & Wang, Y.-K. (2015). Vimentin contributes to epithelial-mesenchymal transition cancer cell mechanics by mediating cytoskeletal organization and focal adhesion maturation. *Oncotarget*, *6*(18), 15966. https://doi.org/10.18632/ONCOTARGET.3862

Lydon, J. P., DeMayo, F. J., Funk, C. R., Mani, S. K., Hughes, A. R., Montgomery, C. A., Shyamala, G., Conneely, O. M., & O'Malley, B. W. (1995). Mice lacking progesterone receptor exhibit pleiotropic reproductive abnormalities. *Genes & Development*, *9*(18), 2266–2278. https://doi.org/10.1101/GAD.9.18.2266

Macias, H., & Hinck, L. (2012). Mammary gland development. *Wiley Interdisciplinary Reviews. Developmental Biology*, *1*(4), 533–557. https://doi.org/10.1002/WDEV.35

Masedunskas, A., Chena, Y., Stussman, R., Weigert, R., & Mather, I. H. (2017). Kinetics of milk lipid droplet transport, growth, and secretion revealed by intravital imaging: lipid droplet release is intermittently stimulated by oxytocin. *Molecular Biology of the Cell*, *28*(7), 935. https://doi.org/10.1091/MBC.E16-11-0776

Mather, I. H., Masedunskas, A., Chen, Y., & Weigert, R. (2019). Symposium review: Intravital imaging of the lactating mammary gland in live mice reveals novel aspects of milk-lipid secretion. *Journal of Dairy Science*, *102*(3), 2760–2782. https://doi.org/10.3168/JDS.2018-15459

McNally, S., & Stein, T. (2017). Overview of Mammary Gland Development: A Comparison of Mouse and Human. *Methods in Molecular Biology*, *1501*, 1–17. https://doi.org/10.1007/978-1-

4939-6475-8_1

Michalczyk, A., Leigh Ackland, M., Brown, R. W., & Collins, J. P. (2001). Lactation affects expression of intermediate filaments in human breast epithelium. *Differentiation; Research in Biological Diversity*, *67*(1–2), 41–49. https://doi.org/10.1046/J.1432-0436.2001.067001041.X

Monks, J., Ladinsky, M. S., & McManaman, J. L. (2020). Organellar Contacts of Milk Lipid Droplets. *Contact (Thousand Oaks (Ventura County, Calif.))*, *3*, 251525641989722. https://doi.org/10.1177/2515256419897226

Mroue, R., Inman, J., Mott, J., Budunova, I., & Bissell, M. J. (2015). Asymmetric Expression of Connexins between luminal epithelial- and myoepithelial- cells is Essential for Contractile Function of the Mammary Gland. *Developmental Biology*, *399*(1), 15. https://doi.org/10.1016/J.YDBIO.2014.11.026

Murrow, L. M., Weber, R. J., Caruso, J. A., McGinnis, C. S., Phong, K., Gascard, P., Rabadam, G., Borowsky, A. D., Desai, T. A., Thomson, M., Tlsty, T., & Gartner, Z. J. (2022). Mapping hormone-regulated cell-cell interaction networks in the human breast at single-cell resolution. *Cell Systems*, *13*(8), 644-664.e8. https://doi.org/10.1016/J.CELS.2022.06.005

Nagasawa, H., & Yanai, R. (1971). Quantitative participation of placental mammotropic hormones in mammary development during pregnancy of mice. *Endocrinologia Japonica*, *18*(6), 507–510. https://doi.org/10.1507/ENDOCRJ1954.18.507

Nazário, A. C., Simões, M. J., & de Lima, G. R. (1994). Morphological and ultrastructural aspects of the cyclical changes of human mammary gland during the menstrual cycle. *Sao Paulo Medical Journal*, *112*(2), 543–547. https://doi.org/10.1590/S1516-31801994000200004

Oakes, S. R., Hilton, H. N., & Ormandy, C. J. (2006). Key stages in mammary gland development: The alveolar switch: Coordinating the proliferative cues and cell fate decisions that drive the formation of lobuloalveoli from ductal epithelium. *Breast Cancer Research*, *8*(2), 1–10. https://doi.org/10.1186/BCR1411/FIGURES/2

Olins, G. M., & Bremel, R. D. (1982). Phosphorylation of myosin in mammary myoepithelial cells in response to oxytocin. *Endocrinology*, *110*(6), 1933–1938. https://doi.org/10.1210/ENDO-110-6-1933

Ostrowska-Podhorodecka, Z., Ding, I., Lee, W., Tanic, J., Abbasi, S., Arora, P. D., Liu, R. S., Patteson, A. E., Janmey, P. A., & McCulloch, C. A. (2021). Vimentin tunes cell migration on collagen by controlling β1 integrin activation and clustering. *Journal of Cell Science*, *134*(6). https://doi.org/10.1242/JCS.254359

Ostrowska-Podhorodecka, Z., Ding, I., Norouzi, M., & McCulloch, C. A. (2022). Impact of Vimentin on Regulation of Cell Signaling and Matrix Remodeling. *Frontiers in Cell and*

*Developmental Biology*, *10*. https://doi.org/10.3389/FCELL.2022.869069

Ostrowska-Podhorodecka, Z., & McCulloch, C. A. (2021). Vimentin regulates the assembly and function of matrix adhesions. *Wound Repair and Regeneration : Official Publication of the Wound Healing Society [and] the European Tissue Repair Society*, *29*(4), 602–612. https://doi.org/10.1111/WRR.12920

Paavolainen, O., & Peuhu, E. (2021). Integrin-mediated adhesion and mechanosensing in the mammary gland. *Seminars in Cell & Developmental Biology*, *114*, 113–125. https://doi.org/10.1016/J.SEMCDB.2020.10.010

Paine, I. S., & Lewis, M. T. (2017). The Terminal End Bud: the Little Engine that Could. *Journal of Mammary Gland Biology and Neoplasia 2017 22:2*, *22*(2), 93–108. https://doi.org/10.1007/S10911-017-9372-0

Parra-Vargas, M., Ramon-Krauel, M., Lerin, C., & Jimenez-Chillaron, J. C. (2020). Size Does Matter: Litter Size Strongly Determines Adult Metabolism in Rodents. *Cell Metabolism*, *32*(3), 334–340. https://doi.org/10.1016/J.CMET.2020.07.014

Pattabiraman, S., Azad, G. K., Amen, T., Brielle, S., Park, J. E., Sze, S. K., Meshorer, E., & Kaganovich, D. (2020). Vimentin protects differentiating stem cells from stress. *Scientific Reports*, *10*(1). https://doi.org/10.1038/S41598-020-76076-4

Patteson, A. E., Pogoda, K., Byfield, F. J., Mandal, K., Ostrowska-Podhorodecka, Z., Charrier, E. E., Galie, P. A., Deptuła, P., Bucki, R., McCulloch, C. A., & Janmey, P. A. (2019). Loss of Vimentin Enhances Cell Motility through Small Confining Spaces. *Small (Weinheim an Der Bergstrasse, Germany)*, *15*(50). https://doi.org/10.1002/SMLL.201903180

Patteson, A. E., Vahabikashi, A., Goldman, R. D., & Janmey, P. A. (2020). Mechanical and Non-Mechanical Functions of Filamentous and Non-Filamentous Vimentin. *BioEssays : News and Reviews in Molecular, Cellular and Developmental Biology*, *42*(11). https://doi.org/10.1002/BIES.202000078

Patteson, A. E., Vahabikashi, A., Pogoda, K., Adam, S. A., Mandal, K., Kittisopikul, M., Sivagurunathan, S., Goldman, A., Goldman, R. D., & Janmey, P. A. (2019). Vimentin protects cells against nuclear rupture and DNA damage during migration. *The Journal of Cell Biology*, *218*(12), 4079–4092. https://doi.org/10.1083/JCB.201902046

Pérez-Sala, D., Oeste, C. L., Martínez, A. E., Carrasco, M. J., Garzón, B., & Cañada, F. J. (2015). Vimentin filament organization and stress sensing depend on its single cysteine residue and zinc binding. *Nature Communications 2015 6:1*, *6*(1), 1–17. https://doi.org/10.1038/ncomms8287

Peuhu, E., Virtakoivu, R., Mai, A., Wärri, A., & Ivaska, J. (2017). Epithelial vimentin plays a

functional role in mammary gland development. *Development (Cambridge)*, *144*(22), 4103–4113. https://doi.org/10.1242/dev.154229

Radisky, D. C., & Hartmann, L. C. (2009). Mammary Involution and Breast Cancer Risk: Transgenic Models and Clinical Studies. *Journal of Mammary Gland Biology and Neoplasia*, *14*(2), 181. https://doi.org/10.1007/S10911-009-9123-Y

Ragueneau, S. (1987). Early development in mice. IV: Quantity and gross composition of milk in five inbred strains. *Physiology & Behavior*, *40*(4), 431–435. https://doi.org/10.1016/0031-9384(87)90027-8

Raymond, K., Cagnet, S., Kreft, M., Janssen, H., Sonnenberg, A., & Glukhova, M. A. (2011). Control of mammary myoepithelial cell contractile function by α3β1 integrin signalling. *The EMBO Journal*, *30*(10), 1896–1906. https://doi.org/10.1038/EMBOJ.2011.113

Richert, M. M., Schwertfeger, K. L., Ryder, J. W., & Anderson, S. M. (2000). An atlas of mouse mammary gland development. *Journal of Mammary Gland Biology and Neoplasia*, *5*(2), 227–241. https://doi.org/10.1023/A:1026499523505

Ridge, K. M., Eriksson, J. E., Pekny, M., & Goldman, R. D. (2022). Roles of vimentin in health and disease. *Genes & Development*, *36*(7–8), 391–407. https://doi.org/10.1101/GAD.349358.122

Schedin, P., & Hovey, R. C. (2010). Editorial: The Mammary Stroma in Normal Development and Function. *Journal of Mammary Gland Biology and Neoplasia*, *15*(3), 275. https://doi.org/10.1007/S10911-010-9191-Z

Schedin, P., & Keely, P. J. (2011). Mammary gland ECM remodeling, stiffness, and mechanosignaling in normal development and tumor progression. *Cold Spring Harbor Perspectives in Biology*, *3*(1), 1–22. https://doi.org/10.1101/CSHPERSPECT.A003228

Schindelin, J., Arganda-Carreras, I., Frise, E., Kaynig, V., Longair, M., Pietzsch, T., Preibisch, S., Rueden, C., Saalfeld, S., Schmid, B., Tinevez, J. Y., White, D. J., Hartenstein, V., Eliceiri, K., Tomancak, P., & Cardona, A. (2012). Fiji: an open-source platform for biological-image analysis. *Nature Methods 2012 9:7*, *9*(7), 676–682. https://doi.org/10.1038/nmeth.2019

Shehata, M., Teschendorff, A., Sharp, G., Novcic, N., Russell, I. A., Avril, S., Prater, M., Eirew, P., Caldas, C., & Watson, C. J. (2012). Phenotypic and functional characterisation of the luminal cell hierarchy of the mammary gland. *Breast Cancer Research*, *14*(5), 1–19. https://doi.org/10.1186/BCR3334/FIGURES/6

Shen, W. J., Patel, S., Eriksson, J. E., & Kraemer, F. B. (2010). Vimentin Is a Functional Partner of Hormone Sensitive Lipase And Facilitates Lipolysis. *Journal of Proteome Research*, *9*(4), 1786. https://doi.org/10.1021/PR900909T

Shen, W. J., Zaidi, S. K., Patel, S., Cortez, Y., Ueno, M., Azhar, R., Azhar, S., & Kraemer, F. B.

(2012). Ablation of vimentin results in defective steroidogenesis. *Endocrinology*, *153*(7), 3249–3257. https://doi.org/10.1210/EN.2012-1048

Slepicka, P. F., Somasundara, A. V. H., & dos Santos, C. O. (2021). The molecular basis of mammary gland development and epithelial differentiation. *Seminars in Cell & Developmental Biology*, *114*, 93–112. https://doi.org/10.1016/J.SEMCDB.2020.09.014

Sonja Vahlman. (2021). *Vimentiini ja ihmisen maitorauhasepiteelin mekanobiologinen säätelyle* [University of Turku]. https://urn.fi/URN:NBN:fi-fe2021082644412

Stemberger, B. H., Walsh, R. M., & Patton, S. (1984). Morphometric evaluation of lipid droplet associations with secretory vesicles, mitochondria and other components in the lactating cell. *Cell and Tissue Research 1984 236:2*, *236*(2), 471–475. https://doi.org/10.1007/BF00214252

Sternlicht, M. D. (2005). Key stages in mammary gland development: The cues that regulate ductal branching morphogenesis. *Breast Cancer Research*, *8*(1), 1–11. https://doi.org/10.1186/BCR1368/TABLES/1

Stevenson, A. J., Vanwalleghem, G., Stewart, T. A., Condon, N. D., Lloyd-Lewis, B., Marino, N., Putney, J. W., Scott, E. K., Ewing, A. D., & Davis, F. M. (2020). Multiscale imaging of basal cell dynamics in the functionally mature mammary gland. *Proceedings of the National Academy of Sciences of the United States of America*, *117*(43), 26822–26832. https://doi.org/10.1073/PNAS.2016905117/SUPPL_FILE/PNAS.2016905117.SM15.MP4

Stockley, P., & Parker, G. A. (2002). Life history consequences of mammal sibling rivalry. *Proceedings of the National Academy of Sciences of the United States of America*, *99*(20), 12932. https://doi.org/10.1073/PNAS.192125999

Strouhalova, K., Přechová, M., Gandalovičová, A., Brábek, J., Gregor, M., & Rosel, D. (2020). Vimentin Intermediate Filaments as Potential Target for Cancer Treatment. *Cancers*, *12*(1). https://doi.org/10.3390/CANCERS12010184

Tortora, G. J., & Bryan, D. (2014). *Principles of Anatomy & Physiology* (14th ed.). Wiley.

Van engeland, nicole A., Suarez Rodriguez, F., Rivero-Müller, A., Ristori, T., Duran, C. L., J A Stassen, O. M., Antfolk, D., Driessen, R. H., Ruohonen, S., Ruohonen, S. T., Nuutinen, S., Savontaus, E., Loerakker, S., Bayless, K. J., Sjöqvist, M., Bouten, carlijn V, Eriksson, J. E., & Sahlgren, cecilia M. (2019). Vimentin regulates notch signaling strength and arterial remodeling in response to hemodynamic stress. *Scientific Reports*, *9*, 12415. https://doi.org/10.1038/s41598-019-48218-w

van Loosdregt, I. A. E. W., Weissenberger, G., van Maris, M. P. F. H. L., Oomens, C. W. J., Loerakker, S., Stassen, O. M. J. A., & Bouten, C. V. C. (2018). The Mechanical Contribution of Vimentin to Cellular Stress Generation. *Journal of Biomechanical Engineering*, *140*(6).

https://doi.org/10.1115/1.4039308

Vannuccini, S., Bocchi, C., Severi, F. M., Challis, J. R., & Petraglia, F. (2016). Endocrinology of human parturition. *Annales d'endocrinologie*, *77*(2), 105–113. https://doi.org/10.1016/J.ANDO.2016.04.025

Vasquez, C. G., & Martin, A. C. (2016). Force Transmission in Epithelial Tissues. *Developmental Dynamics : An Official Publication of the American Association of Anatomists*, *245*(3), 361. https://doi.org/10.1002/DVDY.24384

Vicente-Manzanares, M., Ma, X., Adelstein, R. S., & Horwitz, A. R. (2009). Non-muscle myosin II takes centre stage in cell adhesion and migration. *Nature Reviews. Molecular Cell Biology*, *10*(11), 778–790. https://doi.org/10.1038/nrm2786

Walter, L., Narayana, V. K., Fry, R., Logan, A., Tull, D., & Leury, B. (2020). Milk fat globule size development in the mammary epithelial cell: a potential role for ether phosphatidylethanolamine. *Scientific Reports*, *10*(1). https://doi.org/10.1038/S41598-020-69036-5

Watson, C. J. (2021). How should we define mammary stem cells? *Trends in Cell Biology*, *31*(8), 621–627. https://doi.org/10.1016/J.TCB.2021.03.012

Webb, R. C. (2003). Smooth muscle contraction and relaxation. *Advances in Physiology Education*, *27*(1–4), 201–206. https://doi.org/10.1152/ADVAN.00025.2003

Weymouth, N., Shi, Z., & Rockey, D. C. (2012). Smooth muscle α actin is specifically required for the maintenance of lactation. *Developmental Biology*, *363*(1), 1–14. https://doi.org/10.1016/J.YDBIO.2011.11.002

Wilfling, F., Wang, H., Haas, J. T., Krahmer, N., Gould, T. J., Uchida, A., Cheng, J. X., Graham, M., Christiano, R., Fröhlich, F., Liu, X., Buhman, K. K., Coleman, R. A., Bewersdorf, J., Farese, R. V., & Walther, T. C. (2013). Triacylglycerol synthesis enzymes mediate lipid droplet growth by relocalizing from the ER to lipid droplets. *Developmental Cell*, *24*(4), 384–399. https://doi.org/10.1016/J.DEVCEL.2013.01.013

Wilhelmsson, U., Stillemark-Billton, P., Borén, J., & Pekny, M. (2019). Vimentin is required for normal accumulation of body fat. *Biological Chemistry*, *400*(9), 1157–1162. https://doi.org/10.1515/HSZ-2019-0170/DOWNLOADASSET/SUPPL/J_HSZ-2019-0170_SUPPL.PDF

Wu, H., Shen, Y., Sivagurunathan, S., Weber, M. S., Adam, S. A., Shin, J. H., Fredberg, J. J., Medalia, O., Goldman, R., & Weitz, D. A. (2022). Vimentin intermediate filaments and filamentous actin form unexpected interpenetrating networks that redefine the cell cortex. *Proceedings of the National Academy of Sciences of the United States of America*, *119*(10),

e2115217119. https://doi.org/10.1073/PNAS.2115217119/SUPPL_FILE/PNAS.2115217119.SM01.AVI

Wulf, E., Deboben, A., Bautz, F. A., Faulstich, H., & Wieland, T. (1979). Fluorescent phallotoxin, a tool for the visualization of cellular actin. *Proceedings of the National Academy of Sciences of the United States of America*, *76*(9), 4498–4502. https://doi.org/10.1073/PNAS.76.9.4498

# Appendixes

## Appendix 1: Multiple-comparison p-values of alveoli size per mouse

| | | | | |
|---|---|---|---|---|
| Dunn's multiple comparisons test | Mean rank diff, | Significant? | Summary | Adjusted P Value |
| WT72 vs. WT73 | 786,1 | Yes | **** | <0,0001 |
| WT72 vs. WT1 | -127,1 | No | ns | >0,9999 |
| WT72 vs. WT2 | -523,9 | Yes | ** | 0,0017 |
| WT72 vs. KO44 | -541,1 | Yes | *** | 0,0002 |
| WT72 vs. KO54 | 289,8 | No | ns | >0,9999 |
| WT72 vs. KO55 | -1098 | Yes | **** | <0,0001 |
| WT72 vs. KO56 | 1251 | Yes | **** | <0,0001 |
| WT72 vs. KO57 | 57,37 | No | ns | >0,9999 |
| WT72 vs. KO61 | -1084 | Yes | **** | <0,0001 |
| WT73 vs. WT1 | -913,2 | Yes | **** | <0,0001 |
| WT73 vs. WT2 | -1310 | Yes | **** | <0,0001 |
| WT73 vs. KO44 | -1327 | Yes | **** | <0,0001 |
| WT73 vs. KO54 | -496,4 | No | ns | 0,0939 |
| WT73 vs. KO55 | -1884 | Yes | **** | <0,0001 |
| WT73 vs. KO56 | 465,4 | No | ns | 0,1911 |
| WT73 vs. KO57 | -728,8 | Yes | *** | 0,0004 |
| WT73 vs. KO61 | -1870 | Yes | **** | <0,0001 |
| WT1 vs. WT2 | -396,9 | No | ns | 0,243 |
| WT1 vs. KO44 | -414 | No | ns | 0,1006 |
| WT1 vs. KO54 | 416,8 | No | ns | 0,371 |
| WT1 vs. KO55 | -970,7 | Yes | **** | <0,0001 |
| WT1 vs. KO56 | 1379 | Yes | **** | <0,0001 |
| WT1 vs. KO57 | 184,4 | No | ns | >0,9999 |
| WT1 vs. KO61 | -957,1 | Yes | **** | <0,0001 |
| WT2 vs. KO44 | -17,2 | No | ns | >0,9999 |
| WT2 vs. KO54 | 813,7 | Yes | **** | <0,0001 |
| WT2 vs. KO55 | -573,8 | Yes | *** | 0,0005 |
| WT2 vs. KO56 | 1775 | Yes | **** | <0,0001 |
| WT2 vs. KO57 | 581,3 | Yes | ** | 0,0041 |
| WT2 vs. KO61 | -560,2 | Yes | ** | 0,0096 |
| KO44 vs. KO54 | 830,9 | Yes | **** | <0,0001 |
| KO44 vs. KO55 | -556,6 | Yes | *** | 0,0002 |
| KO44 vs. KO56 | 1793 | Yes | **** | <0,0001 |
| KO44 vs. KO57 | 598,5 | Yes | ** | 0,0011 |
| KO44 vs. KO61 | -543 | Yes | ** | 0,0077 |
| KO54 vs. KO55 | -1388 | Yes | **** | <0,0001 |
| KO54 vs. KO56 | 961,7 | Yes | **** | <0,0001 |
| KO54 vs. KO57 | -232,4 | No | ns | >0,9999 |
| KO54 vs. KO61 | -1374 | Yes | **** | <0,0001 |

| | | | | |
|---|---|---|---|---|
| KO55 vs. KO56 | 2349 | Yes | **** | <0,0001 |
| KO55 vs. KO57 | 1155 | Yes | **** | <0,0001 |
| KO55 vs. KO61 | 13,61 | No | ns | >0,9999 |
| KO56 vs. KO57 | -1194 | Yes | **** | <0,0001 |
| KO56 vs. KO61 | -2336 | Yes | **** | <0,0001 |
| KO57 vs. KO61 | -1141 | Yes | **** | <0,0001 |

## Appendix 2: Periodate-Lysine-Paraformaldehyde-buffer recipe

Periodate-Lysine-Paraformaldehyde(PLP)-buffer was made by mixing 9.4 ml 0.2 M L-lysine (2.924 g dissolved in 100 ml P-buffer, Alfa Aesar, J62225) 9.4 ml P-buffer, 6.25 ml 4% paraformaldehyde (PFA; 16% Formaldehyde Solution (w/v), Thermo Scientific 28908) in PBS and 0.053 g $NaIO_4$ (Sigma-Aldrich, 311448) and adjusting the pH to 7.4.

## Appendix 3: P-buffer recipe

P-buffer was made by mixing 500 ml mQ $H_2O$, 95 ml 0.2 M $NaH_2PO_4$ and 405 ml 0.2 M $Na_2HPO_4$ together and adjusting the pH to 7.4.